AD_____

Award Number: W81XWH-06-1-0148

TITLE: Enhancing Tumor Drug Delivery by Laser-Activated Vascular Barrier Disruption

PRINCIPAL INVESTIGATOR: Bin Chen, Ph.D.
Chong He, Ph.D.

CONTRACTING ORGANIZATION: University of the Sciences in Philadelphia
Philadelphia, PA 19104

REPORT DATE: December 2007

TYPE OF REPORT: Annual

PREPARED FOR: U.S. Army Medical Research and Materiel Command
Fort Detrick, Maryland 21702-5012

REPORT DOCUMENTATION PAGE

Form Approved
OMB No. 0704-0188

1. REPORT DATE	2. REPORT TYPE	3. DATES COVERED
01-12-2007	Annual	30 Nov 2006 – 29 Nov 2007

4. TITLE AND SUBTITLE

Enhancing Tumor Drug Delivery by Laser-Activated Vascular Barrier Disruption

5a. CONTRACT NUMBER

5b. GRANT NUMBER
W81XWH-06-1-0148

5c. PROGRAM ELEMENT NUMBER

6. AUTHOR(S)

Bin Chen, Ph.D., Chong He, Ph.D.

Email: b.chen@usip.edu

5d. PROJECT NUMBER

5e. TASK NUMBER

5f. WORK UNIT NUMBER

7. PERFORMING ORGANIZATION NAME(S) AND ADDRESS(ES)

University of the Sciences in Philadelphia
Philadelphia, PA 19104

8. PERFORMING ORGANIZATION REPORT NUMBER

9. SPONSORING / MONITORING AGENCY NAME(S) AND ADDRESS(ES)
U.S. Army Medical Research and Materiel Command
Fort Detrick, Maryland 21702-5012

10. SPONSOR/MONITOR'S ACRONYM(S)

11. SPONSOR/MONITOR'S REPORT NUMBER(S)

12. DISTRIBUTION / AVAILABILITY STATEMENT
Approved for Public Release; Distribution Unlimited

13. SUPPLEMENTARY NOTES
Original contains colored plates: ALL DTIC reproductions will be in black and white.

14. ABSTRACT An obstacle for successful drug therapy for cancer is the existence of drug delivery barriers, which causes insufficient drug delivery to the tumor tissue. Because of inadequate drug delivery to the tumor tissue, the drug dose has to be increased, which leads to normal tissue toxicity. This delivery problem not only limits the clinical application of existing chemotherapeutics, but also decreases the effectiveness of many new drugs under development for prostate cancer. We found that vascular targeting photodynamic therapy (PDT), a modality involving the combination of a photosensitizer and laser light, is able to disrupt tumor vascular barrier, a significant hindrance to drug delivery. Therefore, tumor accumulation of circulating molecules is significantly enhanced, as demonstrated by intravital fluorescence microscopy and whole-body fluorescence imaging techniques. Immunofluorescence staining of endothelial cytoskeleton structure further indicates microtubule depolymerization, stress actin fiber formation and intercellular gap formation. Based on these results, we propose to use this laser-based therapy to enhance anticancer drug effectiveness. PDT is currently in worldwide multicenter clinical trials for the localized prostate cancer therapy. The available results indicate that PDT employing advanced laser fiber technology and sophisticated light dosimetry is able to treat localized prostate cancer in an effective and safe way. The combination of photosensitization with current chemotherapy or other new drug therapies will greatly improve clinical treatment for localized prostate cancer patients that accounts for more than 90% of total prostate cancer population.

15. SUBJECT TERMS
Photodynamic therapy, verteporfin, tumor vascular targeting, vascular permeability, imaging

16. SECURITY CLASSIFICATION OF:			17. LIMITATION OF ABSTRACT	18. NUMBER OF PAGES	19a. NAME OF RESPONSIBLE PERSON
a. REPORT	b. ABSTRACT	c. THIS PAGE			19b. TELEPHONE NUMBER *(include area code)*
U	U	U	UU	58	USAMRMC

Standard Form 298 (Rev. 8-98)
Prescribed by ANSI Std. Z39.18

Table of Contents

Introduction

An obstacle to successful cancer drug therapy is the existence of drug delivery barriers, which results in insufficient and heterogeneous drug delivery to the tumor tissue. This drug delivery problem not only limits the clinical application of existing chemotherapeutics, but also decreases the effectiveness of many new drugs under development. Photodynamic therapy (PDT), a modality involving the combination of a photosensitizer and laser light, is an established cancer therapy. Over the past years, we have been focusing on studying PDT as a modality for tumor vascular targeting. Our results demonstrate that vascular-targeting PDT can be used to eradicate tumor tissue, and modify vascular barrier function for an enhanced drug delivery as well. This project will study in detail how vascular photosensitization permeabilizes blood vessels and the influence of photodynamic vascular targeting on tumor vascular function and drug delivery. We rely on various imaging modalities to address these questions. The imaging modalities used in this project include both dynamic live animal/cell imaging that is capable of providing longitudinal information in real time and static ex vivo imaging that is able to reveal biological details at high resolution.

Body

Task 1. To investigate the molecular mechanisms by which photosensitization disrupts endothelial barrier function (months 1-12).

(a). Assess the correlation between photosensitization-induced microtubule disassembly and increase in endothelial cell permeability. The purpose of this study is to determine the role of microtubules in photosensitization-induced endothelial barrier function alteration (months 1-4).

We have found that microtubules play an important role in photosensitization-induced endothelial morphological and functional changes. These results have been published in *Clin Cancer Res.* 2006, 10: 917-23.

(b). Elucidate the mechanism by which photosensitization-induced microtubule depolymerization triggers endothelial cell morphological and functional changes. In particular, we will examine whether Rho activation is involved and the downstream Rho/Rho kinase signaling pathway is functional in this process (months 5-12).

We have examined Rho activity after photosensitization treatment in the SVEC-4 endothelial cells. But our results are not consistent and we are still not sure whether Rho/Rho kinase pathway is active after PDT. This is because Rho is a small molecule protein (~20 kDa) and usually only a small percentage of Rho protein will be activated in response to various stimuli (usually less than 5%). We have to use a special pulldown method to detect this active form of Rho protein. We are repeating this experiment by further optimizing our experimental conditions.

We are also determining other signaling pathways that might be involved in PDT-induced endothelial cell morphological changes. As shown in **Fig 1**, myosin light chain kinase (MLCK) is clearly up-regulated. MLCK is an important protein in regulating endothelial contraction. MLCK activation will lead to MLC phosphorylation, which induces cell contraction. We are currently determining the phosphorylation status of MLC following photosensitization treatment. Although this study is going longer than expected, we believe that it should ultimately lead to some novel findings.

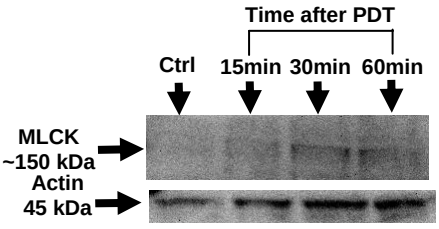

Fig. 1. Western blots of MLCK after photosensitization treatment with verteporfin. The SVEC-4 endothelial cells were treated with 5 mW/cm^2 light for 100 sec after incubation with 200 ng/ml verteporfin for 15 min. Cell lysates were prepared at different time points after treatment.

Task 2. To determine the functional change and the structural basis of photosensitization-induced vascular barrier compromise (months 1-24)

(a). Intravital microscopic study of photosensitization-induced vascular functional changes. Determine tumor hemodynamics, vascular permeability and vessel pore cutoff size changes in the orthotopic MatLyLu prostate tumors after varied doses of photosensitization treatment with verteporfin.

To determine tumor vascular functional changes in real time and at a high resolution, we used intravital fluorescence microscopy, which is able to continuously image both blood vessel morphological and functional changes after vascular-targeting PDT in live animals. To visualize functional blood vessels, we i.v. injected FITC-dextran with a molecular weight of 2000 kDa. Tumor vessel diameter can be measured from FITC-dextran images. To determine tumor blood flow changes, we labeled blood cells with Hoechst dye and measured blood cell velocity changes after PDT. Vascular permeability as well as vessel pore size changes were determined based on the extravasation of fluorochrome-labeled albumin (molecular weight: ~67 kDa) and dextrans with molecular weight of 155 and 2000 kDa.

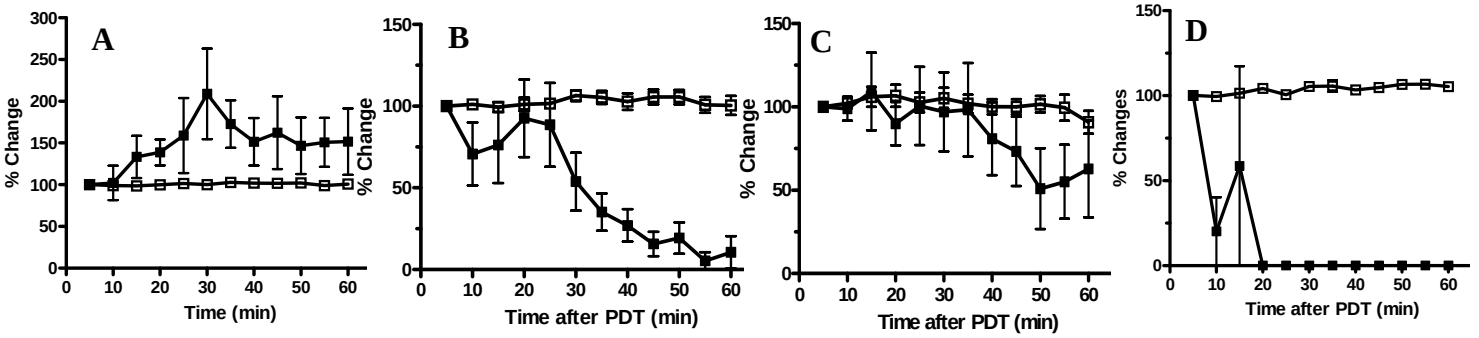

Fig. 2. Tumor blood cell velocity (filled) and vessel diameter (empty) changes after vascular-targeting PDT. The orthotopic MatLyLu rat prostate tumors were treated with vascular-targeting PDT. Immediately after treatment, animals were i.v. injected with 5 mg/kg 2000 kDa FITC-dextran and 20 mg/kg Hoechst and imaged every 5 min up to 60 min after treatment. Vessel diameter were measured based on the 2000 kDa FITC-dextran imaged and blood cell velocity were measured based on the Hoechst images. (A) control tumors without treatment; (B) tumors treated with 50 J/cm^2 at 15 min after 0.25 mg/kg verteporfin (i.v.); (C) tumors treated with 50 J/cm^2 at 15 min after 0.5 mg/kg verteporfin (i.v.); (D) tumors treated with 50 J/cm^2 at 15 min after 1.0 mg/kg verteporfin

As shown in **Fig 2,** vascular-targeting PDT caused dose-dependent decrease in tumor blood flow after treatment. High dose PDT was able to induce sustained blood vessel shutdown with 20 min after treatment. However, there was little change in vessel diameter during the same period of time.

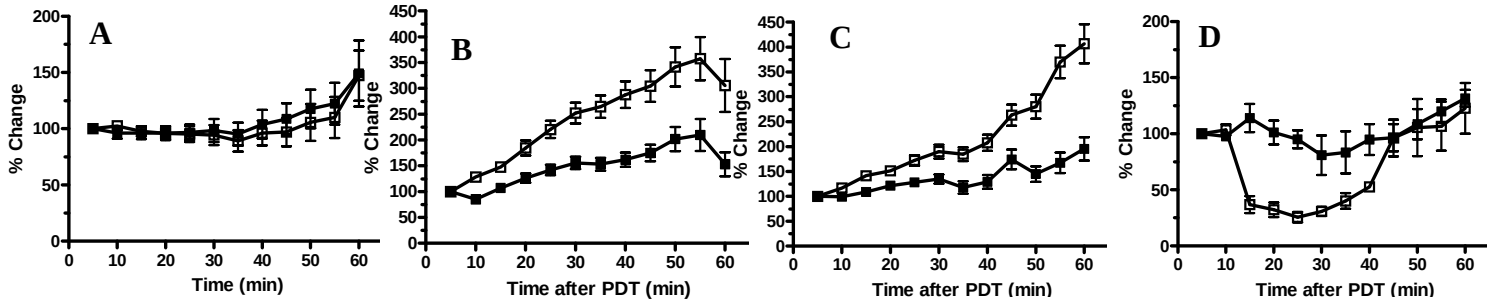

Fig. 3. The extravasation of 2000 kDa FITC-dextran (filled) and 155 kDa TRITC-dextran (empty) after vascular-targeting PDT. The orthotopic MatLyLu rat prostate tumors were treated with vascular-targeting PDT. Immediately after treatment, animals were i.v. injected with 5 mg/kg 2000 kDa FITC-dextran and 10 mg/kg 155 kDa TRITC-dextran and imaged every 5 min up to 60 min after treatment. Region of interest (ROI) was selected on each image and fluorescence intensity in the ROI was measured and plotted. (A) control tumors without treatment; (B) tumors treated with 50 J/cm^2 at 15 min after 0.25 mg/kg verteporfin (i.v.); (C) tumors treated with 50 J/cm^2 at 15 min after 0.5 mg/kg verteporfin (i.v.); (D) tumors treated with 50 J/cm^2 at 15 min after 1.0 mg/kg verteporfin (i.v.).

Fig 3 shows the extravasation of dextran molecules with different molecular weight after different doses of vascular-targeting PDT treatment. PDT treatments with 0.25 and 0.5 mg/kg doses of verteporfin significantly increased tumor uptake of dextran molecules. It appeared that 0.25 mg/kg dose PDT was even stronger in increasing dextran tumor accumulation than the 0.5 mg/kg dose PDT treatment. PDT with 1.0 mg/kg verteporfin failed to enhance dextran tumor accumulation. This is likely because high dose PDT treatments shutdown vascular function shortly after PDT (as shown in **Fig 2**). Therefore, dextran molecules can not be delivered into tumor tissues. Our data also demonstrated that PDT-induced increase in dextran tumor accumulation is dependent upon dextran molecular weight with more significant effect seen in dextran molecules with lower molecular weight.

(b). Assessment of tumor uptake of fluorescence probes with different sizes. This experiment will allow us to evaluate the effect of tumor vascular permeabilization on the delivery of various fluorescence probes with similar sizes to chemotherapeutic agents, antibodies, nanomaterials and gene vectors.

As demonstrated above, vascular functional changes will likely affect tumor uptake of circulating agents. Here we intend to enhance tumor drug delivery by exploiting PDT-induced vascular permeability increase. We have measured tumor uptake of albumin-Evans blue and 2000 kDa FITC-dextran in the MatLyLu rat prostate tumor by using tissue extraction method. Our results demonstrate that photosensitization is able to enhance tumor uptake of these molecules with different molecular weight. These results have been published in *Clin Cancer Res.* 2006, 10: 917-23. As shown in **Fig 3**, although tumor accumulation of both 155 and 2000 kDa dextran molecules can be enhanced by vascular-targeting PDT, lower molecular weight dextran clearly shows a higher enhancement than the one with higher molecular weight.

Since most chemotherapeutic agents tend to be associated with albumin in circulation, we use a whole body fluorescence imaging system to monitor TRITC-albumin tumor uptake in real time on live animals. We found that vascular leakage of fluorescence-labeled albumin (TRITC-albumin) was significantly increased after the vascular-targeting PDT, as compared to the control tumor. This increase in vascular permeability appeared to be dependent upon the PDT dose. Interestingly, PDT-induced increase in TRITC-albumin accumulation was especially pronounced in the tumor periphery. To further confirm these macroscopic imaging results, we sacrificed animals at various time points and excised tumor tissues for fluorescence microscopic study. Similar to the whole body tumor images, TRITC-albumin was found to have more accumulation in the tumor periphery. A revised manuscript based on these results has been submitted to the Int J Cancer (see Appendix 1).

(c). Determine blood vessel structural changes induced by photosensitized vascular permeabilization. Light and electron microscopy and immunohistochemistry technique will be used to examine vessel structural alterations.

We have performed light and electron microscopy to examine vessel structural changes after PDT. At the light microscopy level, we have found that PDT induced vessel dilation and occlusion at early time points after treatment, which progress to severe vessel degeneration and rapture at late times. At the electron microscopy level, we found platelet aggregation, thrombus formation and endothelial cell rupture (**Fig 4**). All these findings suggest that PDT damages endothelial cells, which induce platelet aggregation and vascular shutdown.

We also performed immunohistochemistry to stain vessel endothelial marker CD31, pericyte marker smooth muscle actin and basement membrane marker Type IV collagen. We found that PDT caused a loss of CD31 staining, again suggesting direct endothelial damage. Interestingly, we found that tumor tissues showed spatial variation in the vessel supporting structure. Central blood vessels generally don't have open lumen and have less coverage of vessel supporting structure (Figure 2 in Appendix 2). This might explain the disparity between interior and peripheral vasculature in vascular response to vascular-targeting PDT.

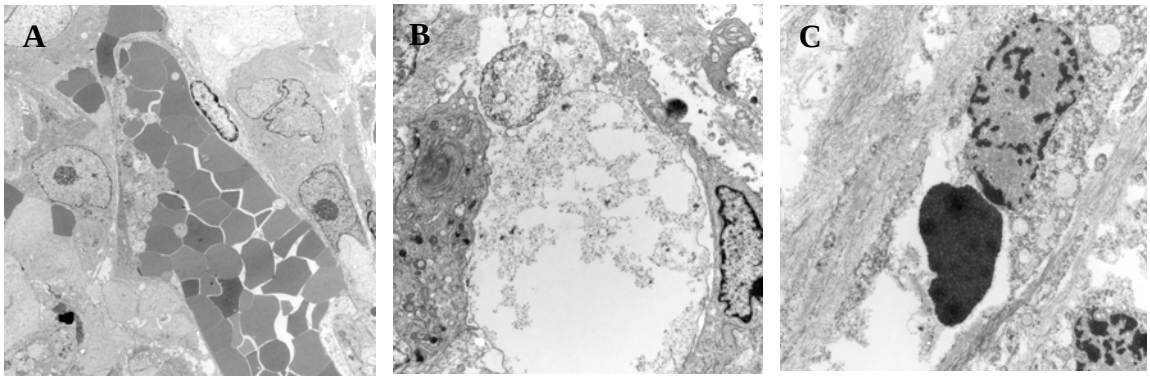

Fig. 4. The electron microscopic photographs showing vascular damage after vascular-targeting PDT. The PC3 human prostate tumors were treated with vascular-targeting PDT (40 J/cm^2 at 15 min after 0.5 mg/kg verteporfin (i.v.)). (A) 1 h after PDT showing platelet aggregation and thrombus formation; (B) 6 h after PDT showing edema, endothelial cell degeneration and vessel rupture; (C) 24 h after PDT showing endothelial cell death, vessel rupture and tumor cell death.

Task 3. To explore the potential of improving tumor drug delivery and therapeutic effect by photosensitized vascular permeabilization (months 25-36).

a. Fluorescence imaging, microscopy & flow cytometry analysis of tumor drug distribution and penetration. Uptake of chemotherapeutic drug mitoxantrone and antibody MDX-H210 (anti-HER2 x CD64) will be quantified by non-invasive whole body fluorescence imaging system, fluorescence microcopy and flow cytometry. Limitation of anticancer drug delivery and enhancement by photosensitized vascular permeabilization will be assessed at whole body, tumor tissue and tumor cell levels.

Antibody MDX-H210 is no longer available for research as the company has discontinued this product. Instead, we have chosen bevacizumab (Avastin) in this project. Bevacizumab is a FDA-approved recombinant humanized monoclonal antibody (MW 149 kDa) that binds to VEGF. We have labeled bevacizumab with Alex Fluor 647 dye using Invitrogen small animal in vivo imaging protein labeling reagents and are examining the influence of verteporfin-PDT on the distribution of bevacizumab.

b. Evaluate tumor response following the combination of anticancer agents (mitoxantrone or MDX-H210) and verteporfin-photosensitization. This study intends to demonstrate that photosensitized vascular permeabilization will lead to a more effective and safer use of conventional chemotherapeutics and new anticancer agent.

We have started to evaluate tumor response following the combination therapy. This is a key experiment for the whole project. We first combined verteporfin-mediated photodynamic therapy with antibody drug bevacizumab in the PC3 human prostate tumor model. As shown in **Fig 5**, the average tumor volume in the group of animals treated with the combination therapy is only about half of the PDT alone group.

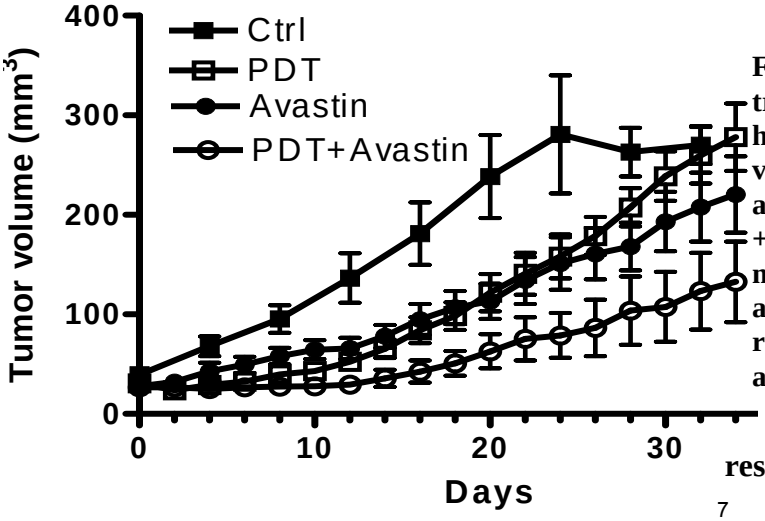

Fig. 5. Tumor regrowth curve after different treatments. For the PDT only group, PC3 human prostate tumors were treated with vascular-targeting PDT (40 J/cm^2 at 15 min after 0.5 mg/kg verteporfin (i.v.)). For the PDT + Ava group, animals were injected with 50 mg/kg Avastin (bevacizumab) immediately after PDT treatment. The control group received no treatment. Each group includes 6-7 animals.

Key research accomplishments

- Photosensitization induces microtubule depolymerization and stress fiber actin formation, leading to endothelial morphological changes and barrier dysfunction.
- Vascular-targeting PDT induces time- and dose-dependent decrease in tumor blood flow and increase in vascular permeability.
- PDT-induced vascular barrier dysfunction leads to increased accumulation of circulating molecules in tumor tissues, which can be used to enhance drug delivery to the tumor tissue. Low dose PDT is more effective in enhancing tumor drug delivery than the high dose PDT and PDT-induced drug delivery enhancement is especially pronounced in the tumor periphery.
- Combination of vascular-targeting PDT and antibody drug bevacizumab (Avastin) results in an enhanced anti-tumor effect.

Reportable outcomes

Publications:

Chen B, Pogue BW, Luna J, Hardman R, Hoopes PJ, Hasan T. Tumor vascular permeabilization by vascular-targeting photosensitization: effects, mechanism and therapeutic implications. *Clin Cancer Res.* 2006, 10: 917-23.

Chen B, Pogue BW, Hoopes PJ, Hasan T. Vascular and cellular targeting for photodynamic therapy. *Crit Rev Eukaryot Gene Expr.* 2006, 16: 279-306.

Chen B, Crane C, He C, Gondek D, Agharkar P, Savellano M, Hoopes PJ, Pogue BW. Disparity between prostate tumor interior versus peripheral vasculature in vascular response to verteporfin-mediated vascular-targeting therapy. *Int J Cancer (revised submission under review).*

Chen B, He C, de Witte P, Hoopes PJ, Hasan T, Pogue BW. "Vascular Targeting in Photodynamic Therapy" in *Advances in Photodynamic Therapy: Basic, Translational and Clinical, Michael R. Hamblin, Editor, by Artech House, Inc. 2008.*

Abstracts:

Chen B, He C, Crane C, Pogue BW. Fluorescence imaging of verteporfin-mediated photodynamic therapy targeting prostate tumor vasculature. *The Department of Defense (DoD) Innovative Minds in Prostate Cancer Today (IMPACT) meeting, Sep 5-8, 2007, Atlanta, Georgia.*

Chen B, He C, Crane C, Agharkar P, Pogue BW. Fluorescence imaging of verteporfin-mediated photodynamic therapy targeting prostate tumor vasculature. *Program & Abstracts of 11th World Congress of the International Photodynamic Association (IPA, March 28-31, 2007, Shanghai, China).*

Chen B, Pogue BW, Hoopes PJ, Hasan T. Effects and mechanisms of vascular permeabilization by vascular-targeting photodynamic therapy. *Conference Proceedings of the 33rd Meeting of the American Society for Photobiology (Jul 8-12, 2006, Puerto Rico).*

Conclusions

We have found that photodynamic tumor vascular targeting induced significant vascular morphological and functional changes. As a result, tumor accumulation of fluorescence molecular probes with different molecular weight is significantly enhanced after photodynamic vascular targeting. The combination of photodynamic tumor vascular targeting and anticancer agents leads to a synergistic therapeutic effect.

Appendices

Chen B, Crane C, He C, Gondek D, Agharkar P, Savellano M, Hoopes PJ, Pogue BW. Disparity between prostate tumor interior versus peripheral vasculature in vascular response to verteporfin-mediated vascular-targeting therapy. *Int J Cancer (revised submission under review).*

Chen B, He C, de Witte P, Hoopes PJ, Hasan T, Pogue BW. "Vascular Targeting in Photodynamic Therapy" in *Advances in Photodynamic Therapy: Basic, Translational and Clinical, Michael R. Hamblin, Editor, by Artech House, Inc. 2008.*

Disparity between prostate tumor interior versus peripheral vasculature in response to verteporfin-mediated vascular-targeting therapy

Running title: Disparity in vascular response to verteporfin-PDT

Bin Chen[1, 2*], Curtis Crane[3], Chong He[1], David Gondek[4], Priyanka Agharkar[1], Mark Savellano[3], P. Jack Hoopes[3, 5], Brian W. Pogue[3, 5, 6]

[1]Department of Pharmaceutical Sciences, Philadelphia College of Pharmacy, University of the Sciences in Philadelphia, Philadelphia, PA 19104; [2]Department of Radiation Oncology, University of Pennsylvania, Philadelphia, PA 19104; [3]Department of Surgery, Dartmouth Medical School, Lebanon, NH 03756; [4]Department of Immunology, Dartmouth Medical School, Lebanon, NH 03756; [5]Thayer School of Engineering, Dartmouth College, Hanover, NH 03755; [6]Wellman Center for Photomedicine, Massachusetts General Hospital, Department of Dermatology, Harvard Medical School, Boston, MA 02114.

***Corresponding author:** Bin Chen, Ph.D., Department of Pharmaceutical Sciences, Philadelphia College of Pharmacy, University of the Sciences in Philadelphia, 600 South 43rd Street, Philadelphia, PA 19104. Tel: 215-596-7481; Fax: 215-895-1161; Email: b.chen@usip.edu.

Key words: photodynamic therapy (PDT), verteporfin, vascular targeting, fluorescence imaging, vascular permeability, tumor perfusion, enhanced green fluorescence protein (EGFP), prostate tumor model.

Journal category: Cancer Therapy

Brief description: *In vivo* animal and *ex vivo* tumor fluorescence imaging showed tumor microcirculation disruption and tumor cell death caused by vascular-targeting photodynamic therapy (PDT) with verteporfin. However, peripheral blood vessels were found less responsive to PDT-induced vascular shutdown than interior blood vessels.

Abstract

Photodynamic therapy (PDT) is a light-based cancer treatment modality. Here we employed both *in vivo* and *ex vivo* fluorescence imaging to visualize vascular response and tumor cell survival after verteporfin-mediated PDT designed to target tumor vasculature. The EGFP-MatLyLu prostate tumor cells, transduced with EGFP using lentivirus vectors, were implanted in the athymic nude mice. Immediately after PDT with different doses of verteporfin, tumor-bearing animals were injected with a fluorochrome-labeled albumin. The extravasation of fluorescent albumin along with tumor EGFP fluorescence was monitored non-invasively with a whole-body fluorescence imaging system. *Ex vivo* fluorescence microscopy was performed on frozen sections of tumor tissues taken at different times after treatment. Both *in vivo* and *ex vivo* imaging demonstrated that vascular-targeting PDT with verteporfin significantly increased the extravasation of fluorochrome-labeled albumin in the tumor tissue especially in the tumor periphery. Although PDT induced substantial vascular shutdown in interior blood vessels, some peripheral tumor vessels were able to maintain perfusion function up to 24 hours after treatment. As a result, viable tumor cells were typically detected in the tumor periphery in spite of extensive tumor cell death. Our results demonstrated that vascular-targeting PDT with verteporfin caused a dose- and time-dependent increase in vascular permeability and decrease in blood perfusion. However, as compared to the interior blood vessels, peripheral tumor blood vessels were found less sensitive to PDT-induced vascular shutdown, which is responsible for subsequent tumor recurrence in the tumor periphery.

Introduction

Photodynamic therapy (PDT) induces tumor destruction through a photochemical reaction involving a photosensitizer, light of a specific wavelength matching the absorption wavelength of the photosensitizer, and the molecular oxygen [1]. Singlet oxygen, a product of this photochemical reaction, is mainly responsible for the biological effects of PDT by causing oxidative damage to the target cells and tissues [2]. Although direct tumor cyotoxicity and immune response are involved as well, damage to the tumor vasculature has been shown to contribute significantly to the overall PDT effect with most photosensitizers [3].

Verteporfin (the lipid-formulation of benzoporphyrin derivative monoacid ring A) is a photosensitizer that is currently approved for the treatment of age-related macular degeneration (AMD) [4]. We have shown previously the dynamic distribution of verteporfin from being predominantly intravascular at 15 minutes after intravenous injection to being mainly extravascular at 3 hours after injection [5]. Based on this pharmacokinetic property, preferential tumor vascular targeting can be achieved by illumination at 15 minutes after verteporfin administration. We have been exploring this passive vascular targeting principle for the treatment of prostate tumors. Intravital fluorescence microscope study in the MatLyLu rat prostate tumor model demonstrates that vascular-targeting PDT with verteporfin induces vascular permeability increase and thrombus formation, which ends in vascular shutdown and tumor necrosis [6]. These results indicate that vascular-targeting PDT using verteporfin can be used for the management of localized prostate cancer.

Since vascular damage is the dominant effect of PDT, vascular-targeting PDT in particular, it is important to study in detail how photosensitization modifies vascular functions. Most studies on PDT-induced tumor vascular changes have been done on excised tumor specimens after

sacrificing the animals. Although rich in revealing microscopic details, such studies are only able to provide snap-shot information on each individual animal. To obtain longitudinal information in a single animal, non-invasive imaging techniques are necessary to examine vessel functional changes after PDT. As a matter of fact, imaging modalities such as laser Doppler perfusion imaging [7, 8], diffuse correlation spectroscopy [9], laser speckle imaging [10, 11], optical coherence tomography [12] and ultrasonography [13] have all been shown to be able to monitor tumor blood flow dynamics non-invasively after PDT. Moreover, non-invasive imaging using contrast agents can not only follow perfusion changes, but also provide real-time information regarding vascular permeability. For instance, angiography with fluorescence dye fluorescein or indocyanine green is routinely used to examine vessel leakage and occlusion in AMD patients treated with PDT [14]. Changes in tumor perfusion and vascular permeability after PDT have also been studied with contrast-enhanced MRI [15, 16].

Being highly sensitive and versatile, *in vivo* fluorescence imaging is able to provide both macroscopic and microscopic longitudinal data in individual animals which cannot be obtained in other ways [17-19]. In this study, we report the use of an *in vivo* whole-body fluorescence imaging system to monitor vascular response to verteporfin-PDT and tumor cell survival after treatment in an EGFP-transduced prostate tumor model. We also compared the *in vivo* tumor imaging study with the *ex vivo* fluorescence microscopy of frozen tumor sections. Our results indicated the difference between tumor interior versus peripheral blood vessels in vascular response to the vascular-targeting PDT.

Materials and Methods

Production & titer of lentivirus. Lentiviral production was performed as described [20]. Briefly, we co-transfected pWPT-EGFP and third-generation packaging vectors into 293FT cells (Invitrogen Life Technologies) and collected culture supernatants after 48 and 72 h of incubation in 37°C and 5% CO_2 incubator. We recovered virus by ultracentrifugation (1.5 h at 25,000 rpm) in a Beckman SW28 rotor and resuspended the virus pellet in 25 ul of Opt-MEM media (Invitrogen Life Technologies). Viral titers were determined by infecting 293FT cells with serial dilutions of concentrated lentivirus followed by flow cytometry analysis 48 h later. Typical viral preparations yielded 5×10^8 transducing units (TU)/ml.

Tumor cells & lentiviral transduction. R3327-MatLyLu rat prostate cancer cells were maintained in the RPMI-1640 medium with glutamine (Mediatech, Herndon, VA) supplemented with 10% fetal bovine serum (HyClone, Logan, UT) and 100 units/ml penicillin-streptomycin (Mediatech) at 37°C in a 5% CO_2 incubator. For lentiviral transduction, the MatLyLu cells were infected with a multiplicity of infection (MOI) of 50 and allowed to incubate overnight. Polybrene (8 ug/ml, Sigma) was used to facilitate lentiviral transduction. Supernatant was then removed after infection and replaced with completed RPMI-1640 growth medium. EGFP-transduced MatLyLu cells were examined with a fluorescence microscope at 48 h after transduction. EGFP-MatLyLu cells were harvested, serial diluted and implanted in the 96-well plate with the cell density of 1 cell per well. After the incubation of 7 days at 37°C and 5% CO_2 atmosphere, the clone exhibiting the highest EGFP fluorescence intensity was selected and expanded for the subsequent experiments.

Animals & tumor models. Male NCr athymic nude mice (4-5 weeks old, National Cancer Institute, Frederick, MD) were used throughout the study. Tumors were induced by subcutaneous injection of about 1×10^5 EGFP-MatLyLu tumor cells in the thigh region of mice. Tumors were used for experiments when reaching a size of 5-7 mm in diameter. All animal procedures were carried out according to a protocol approved by the Institutional Animal Care and Use Committee (IACUC).

Photosensitizer. Verteporfin (benzoporphyrin derivative (BPD) in a lipid-formulation) was obtained from QLT Inc. (Vancouver, Canada) as a gift. A stock saline solution of verteporfin was reconstituted according to the manufacturer's instructions and stored at 4°C in the dark.

PDT Treatments. A diode laser system (High Power Devices Inc., North Brunswick, NJ) at 690 nm wavelength was used throughout this study for the irradiation of EGFP-MatLyLu tumors. The laser was coupled to an optical fiber with 600 μm core diameter and expanded to generate an 11 mm-diameter illumination spot through a collimator. Animals were anesthetized with injection (i.p.) of a mixture of ketamine (90 mg/kg) and xylazine (9 mg/kg) and tumors were exposed to light with an irradiance of 50 mW/cm^2. Light intensity was measured with an optical power meter (Thorlabs Inc, North Newton, NJ). Verteporfin was injected (i.v.) at a dose of 0.25 mg/kg, at 15 min prior to light irradiation.

Non-invasive tumor fluorescence imaging & image analysis. Tumor-bearing animals were i.v. injected with 20 mg/kg albumin labeled with tetramethylrhodamine isothiocyanate (TRITC-albumin, Sigma) immediately after PDT. EGFP-MatLyLu tumors were imaged with a non-invasive whole body tumor fluorescence imaging system for the EGFP and TRITC signal before and after treatment. The setup of this self-built broad beam imaging system has been described in detail in our previous paper [21]. Briefly, the system includes a filtered white light source for

excitation and a SensiCamQE high performance digital CCD camera (The Cook Corp, Auburn Hills, MI) to capture fluorescence emission passing through an emission filter. We used a 470/20 nm excitation filter and a 520/20 nm emission filter for the EGFP imaging; and a 535/20 nm excitation filter and 590 nm long-pass emission filter for the TRITC imaging. The camera settings were kept constant for the control and PDT-treated animals throughout the imaging process. Animals were anesthetized by inhaling 1.5% isofluorane during imaging.

To analyze the images, a circular region of interest (ROI) with 2.5 mm in diameter was selected over tumor or tumor-adjacent normal tissue area on the fluorescence images. The EGFP and TRITC fluorescence intensity in the ROI was quantified using the NIH ImageJ software. The fluorescence intensity in the tumor or tumor-adjacent tissue after PDT was normalized to its own pretreatment value in each animal and the data from different animals were pooled to generate response curves.

Tumor tissue fluorescence microscopy. Tumor-bearing animals were i.v. injected with 20 mg/kg Hoechst (Sigma) as a vascular perfusion marker at different time points after treatment. Animals were euthanized within 1 minute after injection and tumor tissues were excised and snap-frozen in isopentane pre-cooled with liquid nitrogen. Frozen tumor sections with thickness of 10 um were cut and examined under a Leica DMI6000B fluorescence microscope with the appropriate filter set for Hoechst (Excitation: 360/40 nm; Emission: 470/40 nm) and TRITC (Excitation: 546/12 nm; Emission: 600/40 nm).

Tumor volume measurement & tumor histology. Three dimensional tumor sizes were measured regularly after treatment by a caliper and the tumor volume was calculated using the formula of ($\pi/6 \times$ tumor length $\times$ tumor width $\times$ tumor height). Animals were euthanized at varied time points after treatment. Tumor tissues were excised and fixed in 4% formalin solution.

Fixed tumor tissues were dehydrated and then embedded in paraffin. Tissue sections with thickness of 5 um were cut and stained with H&E.

Results

The extravasation of TRITC-albumin, as indicated by the increase of TRITC fluorescence, was imaged non-invasively with a whole-body fluorescence imaging system. Figure 1 shows the TRITC fluorescence images (red) merged with tumor EGFP images (green) at different time points after vascular-targeting PDT with verteporfin. It can be seen clearly that PDT caused an increase in the TRITC fluorescence, especially in the peri-tumor area. The increase of the TRITC-albumin extravasation induced by PDT appeared to be dose dependent because 50 J/cm^2 light dose PDT led to more increase in the TRITC fluorescence intensity than the 25 J/cm^2 light dose treatment.

To quantify the changes of fluorescence intensity, a circular ROI with 2.5 mm in diameter was placed on the tumor area or tumor-adjacent normal tissue area on the fluorescence images and average TRITC and EGFP fluorescence intensities were quantified using NIH ImageJ software. We found that the average TRITC fluorescence in the tumor area was about 20% lower than the tumor-adjacent normal tissue area presumably due to the high blood volume in the tumor tissue. To illustrate the relative TRITC fluorescence intensity change in the tumor area and adjacent normal tissue area after PDT treatment, we normalized fluorescence intensity values after treatment to their own pretreatment values in each animal. Figure 2 indicates that the TRITC fluorescence signal increases significantly as a function of time following different dose PDT treatments in both tumor (Figure 2a) and tumor-adjacent areas (Figure 2b). The increase in the fluorescence intensity started at about 30 minutes after PDT and reached a plateau around 4

hours after treatment. In both tumor and tumor-adjacent areas, PDT with 50 J/cm^2 light dose induced more increase in the TRITC fluorescence intensity than the 25 J/cm^2 light treatment (P<0.01). The 25 J/cm^2 light dose PDT caused a similar increase (about 1.5-fold increase) in the TRITC fluorescence intensity in the tumor and tumor-adjacent areas (P>0.05). In the case of 50 J/cm^2 PDT, TRITC fluorescence increase in the tumor-adjacent tissue after PDT (about 3-fold increase) was significantly more than the increase in the tumor area (about 2-fold increase, P<0.05). As compared to the control tumor, both 25 and 50 J/cm^2 dose PDT treatments caused a significant decrease in tumor EGFP fluorescence (P<0.01) after treatment (Figure 2c). However, it was noted that, following a decrease in the EGFP fluorescence shortly after PDT, there was no further decrease up to 5 hours after PDT.

To determine the TRITC-albumin distribution in relation to tumor EGFP fluorescence, the TRITC and EGFP intensity was measured along a line drawn through the tumor tissue on the fluorescence images. Figure 3 indicates that the TRITC fluorescence intensity in the peripheral tumor area was higher than in the interior tumor area at 4 hours after injection of TRITC-albumin. However, an opposite pattern was found in tumor EGFP intensity profile where higher intensity values were typically detected in the tumor center. Both 25 and 50 J/cm^2 PDT treatments caused an overall increase in the TRITC intensity and decrease in tumor EGFP intensity. The increase in the TRITC intensity was found to be higher in the peripheral tumor area than in the interior tumor area.

To confirm the whole-body fluorescence imaging results, we euthanized animals at 1, 4 and 24 hours after 50 J/cm^2 PDT treatment and excised tumor tissues for fluorescence microscopic study. To highlight the functional blood vessels, we i.v. injected Hoechst dye shortly before euthanizing the animal. As shown in Figure 4, the functional blood vessels (Hoechst positive

staining) decreased significantly after vascular-targeting PDT with 50 J/cm^2 light dose, as compared to the control tumor. Moreover, functional blood vessels were mainly detected at tumor peripheral areas after PDT. In agreement with the macroscopic tumor imaging results, fluorescence microscopic imaging also demonstrated a significant increase in the TRITC fluorescence intensity after PDT, especially in the tumor periphery.

Tumor response to vascular-targeting PDT was monitored non-invasively by whole body fluorescence imaging. To make tumor cells visible, the MatLyLu tumor cells were transduced with EGFP using lentiviral vectors. The EGFP-MatLyLu tumors were imaged for EGFP fluorescence before and after treatment and representative tumor EGFP fluorescence images were shown in Figure 5. Control tumors grew rapidly and generally exhibited central necrosis when tumor reached about 8-10 mm in diameter. Because dead EGFP-MatLyLu tumor cells were not able to produce EGFP, dead tumor tissues appeared to be dark areas in the EGFP fluorescence images. Although PDT with 25 J/cm^2 light dose induced a partial tumor necrosis, this PDT condition failed to inhibit tumor growth. Actually, tumor growth was even faster than the control tumors (Figure 5 & 6). In contrast, the 50 J/cm^2 PDT was very effective in eradicating prostate tumors, as indicated by a significant decrease in the EGFP fluorescence after treatment (Figure 5). Little EGFP fluorescence was detected by 2 days after PDT. However, this PDT treatment could not cure the animals. Small EGFP fluorescent spots, indicating the existence of viable tumor cells, were often found at tumor edges several days after treatment and gradually grew in size, which finally led to tumor recurrence. As shown in Figure 7, some viable tumor cells were detected histologically at the tumor periphery at 48 hours after 50 J/cm^2 PDT.

Discussion

A whole-body animal fluorescence imaging system was used in this study to visualize non-invasively tumor response to PDT targeting tumor blood vessels in an EGFP-transduced MatLyLu prostate tumor model. The TRITC-albumin was used as a macromolecular probe to image tumor vascular barrier function (vascular permeability). The increase in the TRITC fluorescence intensity, as a result of enhanced extravasation from blood vessels, is an indicator of vascular barrier dysfunction. Since albumin has a plasma half-life of more than 24 hours [22], it can be used to follow vascular permeability changes up to hours after treatment. Tumor EGFP fluorescence was monitored to indicate tumor cell survival because only viable EGFP-MatLyLu tumor cells were able to continuously synthesize EGFP and emit fluorescence. By imaging and measuring the TRITC and EGFP fluorescence, we were able to obtain information of vascular barrier function and tumor cell viability non-invasively in live animals.

We found in the present study that vascular-targeting PDT increased vascular permeability in a dose-dependent manner, which is in agreement with our previous study and confirms that tumor vasculature is the primary target of PDT with verteporfin [6]. Importantly, our results indicated that the enhanced TRITC-albumin tumor uptake as a result of PDT-induced permeability increase was not homogeneous in the tumor tissue. Both *in vivo* and *ex vivo* tumor imaging studies demonstrated that the increase in TRITC-albumin tumor uptake was higher in the peripheral tumor area than in the interior tumor area after PDT. Because the accumulation of a circulating molecule in the tumor tissue is dependent upon the existence of functional blood vessels, this preferential enhancement of TRITC-albumin accumulation in the tumor periphery is likely related to the predominant localization of functional blood vessels in the tumor periphery after

vascular-targeting PDT. As shown in Figure 4, PDT was remarkably effective in inducing interior tumor blood vessel shutdown while some peripheral vessels were still functional even at 24 h after PDT. The early closure of central tumor vessels would limit the enhancement of TRITC-albumin distribution in the tumor center, whereas the prolonged perfusion of some peripheral tumor vessels would allow more TRITC-albumin to continuously extravasate and distribute in the tumor periphery. Although we and others have previously reported that peripheral tumor vessels tend to maintain perfusion function after vascular-targeting PDT [23-25], our present results demonstrated that, even though still functional, these peripheral blood vessels exhibited high vascular permeability due to PDT-induced vascular damage. The existence of these functional blood vessels in the tumor periphery, as a result of disparity in vascular response to PDT between peripheral and interior blood vessels, was apparently associated with peripheral tumor cell survival after PDT. As shown in Figure 7, H&E staining indicated a rim of viable tumor cells in tumor periphery at 48 h after PDT in spite of extensive tumor necrosis. *In vivo* tumor fluorescence imaging demonstrated that the survival of these peripheral tumor cells finally resulted in peripheral tumor recurrence.

It is still not clear why peripheral tumor blood vessels react somewhat differently from interior blood vessels to the vascular-targeting PDT. Understanding the mechanism behind this disparity in vascular response will help to find ways to enhance the therapeutic effects of vascular-targeting PDT. Differences in vascular structure and function between tumor peripheral and interior blood vessels caused by morbid tumor pathobiology possibly contribute to such variations in the vascular response. It is known that tumor tissues have higher tissue interstitial pressure than normal tissues because of leaky tumor blood vessels and lymphatic system malfunction [26, 27]. High tumor interstitial pressure is able to compress tumor vessels and even

cause vessel collapse. This vessel compression/collapse effect is more severe in the tumor interior where tumor interstitial pressure is higher [28, 29]. PDT has been shown to further increase tumor interstitial pressure as a result of enhancing vascular permeability [30, 31]. Such an increase in tumor interstitial pressure will likely impose a greater compression on tumor blood vessels and cause vascular shutdown, especially in tumor interior areas. Moreover, we recently found that, compared to the interior tumor vessels, peripheral tumor blood vessels were generally larger, showed vascular lumen and more coverage of vascular pericytes and basement membrane [32]. Therefore, less mechanic compression together with more vessel supporting structures might make peripheral tumor vessels more resistant than the interior vessels to vessel closure induced by vascular-targeting PDT.

The survival of peripheral tumor cells as a consequence of disparity in vascular response between peripheral and interior blood vessels represents a therapeutic challenge for the vascular-targeting PDT. Several strategies can be adopted to eliminate or at least minimize the surviving tumor cells at the tumor periphery. First of all, we will increase the PDT dose to determine whether a higher dose of vascular-targeting PDT will lead to the shutdown of both interior and peripheral tumor blood vessels, resulting in an increased tumor cure. Secondly, as combination therapies have been routinely used in cancer treatments, one approach of enhancing photodynamic vascular targeting effectiveness is to combine it with other cancer therapies. Combination therapies can be designed based on different targeting principles. Targeting both tumor vascular and cellular compartments by combining vascular-targeting PDT with a cancer cell-targeted therapy can be a promising strategy because the increased vascular permeability induced by PDT can be exploited to enhance anticancer drug delivery [6, 33, 34]. Our present study further demonstrated that the enhancement of drug accumulation mainly occurred at the tumor

periphery where tumor cell survival tends to occur after vascular-targeting PDT. Therefore, combining vascular-targeting PDT with other anticancer drug therapies will allow more anticancer agents to be preferentially deposited in the peripheral tumor area to kill tumor cells that otherwise will survive PDT treatment. This spatial cooperation in tumor cell killing between a vasculature-targeted therapy and a tumor cell-targeted therapy has been shown to achieve a better treatment outcome [5].

Another important combination strategy is to target the surviving and repairing pathways which endothelial cells as well as tumor cells depend on to maintain their survival after vascular-targeting PDT. An example in this case is the combination of vascular-targeting PDT with antiangiogenic therapy. PDT treatments have been shown to stimulate angiogenesis and tumor growth by inducing VEGF upregulation [35, 36]. Depending on the photosensitizer, the type of tumor model and treatment conditions, the elevation of VEGF can be caused by hypoxia-induced HIF-1 activation [35], COX-2 overexpression [37, 38] and p38 MAPK activation [36]. Thus, combined treatments of PDT with VEGF antibody bevacizumab [39], antiangiogenic drug TNP-470 [40] or COX-2 inhibitor [37] have all been shown to enhance the therapeutic effects. As our understanding regarding tumor/endothelial cell adaptation to therapeutic stressors increases, more such rationale-designed combination regimens will be designed to target crucial cellular and molecular surviving pathways, leading to a synergistic treatment outcome.

Because of its stability and easy detection, fluorescence proteins are commonly used to label tumor cells to allow non-invasive imaging of tumor growth, tumor-host interaction and tumor response to therapy in living animals [18]. In the present study, we used EGFP as an indicator of tumor cell viability with the assumption that dead tumor cells are not able to emit EGFP fluorescence. However, because EGFP has a half-life of more than 3 h [41], monitoring EGFP

fluorescence shortly after treatment could not accurately report tumor cell viability. The observed decrease in EGFP fluorescence immediately after PDT was most likely due to the oxidative degradation of EGFP during PDT. This was supported by the fact that there was little further decrease in fluorescence intensity over the next 5 h after PDT (Figure 2c). Although EGFP chromophore formation is dependent upon the availability of molecular oxygen, it has been shown at least *in vitro* that only anoxic conditions (with oxygen concentration less than 0.06%), which induce cell viability decrease, is able to decrease EGFP fluorescence by impairing protein maturation and hypoxia (with oxygen concentration from 0.06-6%) has no significant effect on EGFP fluorescence [42]. Thus, EGFP can be a suitable reporter of tumor cell viability for the evaluation of cancer therapy as long as sufficient time is allowed for the degradation of EGFP produced before treatment.

The imaging system used in this study belongs to a reflectance fluorescence imaging system. Although widely used, this technology comes with some inherent limitations [19]. First of all, due to limited light penetration and strong photon scattering in tissues, it has limited depth of imaging and therefore can not resolve fluorescence signals from different depths of tissue. To circumvent this limitation, we combined this *in vivo* imaging study with the standard *ex vivo* fluorescence microscopy on frozen tissue sections to reveal information in the whole tumor tissue. Secondly, reflectance fluorescence imaging is sensitive to target tissue optical properties (e.g. absorption, scattering, etc), tissue geometry and surrounding tissue optical properties [21]. Thus, fluorescence intensity is dependent upon tissue fluorochrome concentration only if there is little change in these parameters. However, it is very difficult, if not impossible, to control these parameters in imaging tumor response to therapy because tumor volume, blood content (e.g. hemorrhage, vessel dilatation and constriction) and tissue water concentration (e.g. edema) are

all likely to change after therapy. In this case, reflectance fluorescence imaging modality can only provide semi-quantitative information. Nevertheless, a significant advantage of this imaging modality is its capability to perform non-invasive imaging in live animals, which allows us to visualize longitudinal tumor response to PDT in each animal. As demonstrated in the present study, the integration of *in vivo* fluorescence imaging study with *ex vivo* tissue fluorescence microscopy study is able to provide important insights into the effects and mechanisms of photo-activated tumor vascular targeting.

Acknowledgement

This work was supported by Department of Defense (DOD) Prostate Cancer Research Grant W81XWH-06-1-0148. The authors would like to gratefully acknowledge Dr. Tayyaba Hasan from Wellman Center for Photomedicine for helpful discussions and QLT Inc. for providing the verteporfin.

References

1. Dougherty TJ, Gomer CJ, Henderson BW, Jori G, Kessel D, Korbelik M, Moan J, Peng Q. Photodynamic therapy. J Natl Cancer Inst 1998;90:889-905.

2. Schmidt R. Photosensitized generation of singlet oxygen. Photochem Photobiol 2006;82:1161-77.

3. Chen B, Pogue BW, Hoopes PJ, Hasan T. Vascular and cellular targeting for photodynamic therapy. Crit Rev Eukaryot Gene Expr 2006;16:279-305.

4. Brown SB, Mellish KJ. Verteporfin: a milestone in opthalmology and photodynamic therapy. Expert Opin Pharmacother 2001;2:351-61.

5. Chen B, Pogue BW, Hoopes PJ, Hasan T. Combining vascular and cellular targeting regimens enhances the efficacy of photodynamic therapy. Int J Radiat Oncol Biol Phys 2005;61:1216-26.

6. Chen B, Pogue BW, Luna JM, Hardman RL, Hoopes PJ, Hasan T. Tumor vascular permeabilization by vascular-targeting photosensitization: effects, mechanism, and therapeutic implications. Clin Cancer Res 2006;12:917-23.

7. Liu DL, Svanberg K, Wang I, Andersson-Engels S, Svanberg S. Laser Doppler perfusion imaging: new technique for determination of perfusion and reperfusion of splanchnic organs and tumor tissue. Lasers Surg Med 1997;20:473-9.

8. Enejder AM, af Klinteberg C, Wang I, Andersson-Engels S, Bendsoe N, Svanberg S, Svanberg K. Blood perfusion studies on basal cell carcinomas in conjunction with photodynamic therapy and cryotherapy employing laser-Doppler perfusion imaging. Acta Derm Venereol 2000;80:19-23.

9. Yu G, Durduran T, Zhou C, Wang HW, Putt ME, Saunders HM, Sehgal CM, Glatstein E, Yodh AG, Busch TM. Noninvasive monitoring of murine tumor blood flow during and after photodynamic therapy provides early assessment of therapeutic efficacy. Clin Cancer Res 2005;11:3543-52.

10. Kruijt B, de Bruijn HS, van der Ploeg-van den Heuvel A, Sterenborg HJ, Robinson DJ. Laser speckle imaging of dynamic changes in flow during photodynamic therapy. Lasers Med Sci 2006;21:208-12.

11. Smith TK, Choi B, Ramirez-San-Juan JC, Nelson JS, Osann K, Kelly KM. Microvascular blood flow dynamics associated with photodynamic therapy, pulsed dye laser irradiation and combined regimens. Lasers Surg Med 2006;38:532-9.

12. Aalders MC, Triesscheijn M, Ruevekamp M, de Bruin M, Baas P, Faber DJ, Stewart FA. Doppler optical coherence tomography to monitor the effect of photodynamic therapy on tissue morphology and perfusion. J Biomed Opt 2006;11:044011.

13. Ohlerth S, Laluhova D, Buchholz J, Roos M, Walt H, Kaser-Hotz B. Changes in vascularity and blood volume as a result of photodynamic therapy can be assessed with power Doppler ultrasonography. Lasers Surg Med 2006;38:229-34.

14. Schmidt-Erfurth U, Niemeyer M, Geitzenauer W, Michels S. Time course and morphology of vascular effects associated with photodynamic therapy. Ophthalmology 2005;112:2061-9.

15. Zilberstein J, Schreiber S, Bloemers MC, Bendel P, Neeman M, Schechtman E, Kohen F, Scherz A, Salomon Y. Antivascular treatment of solid melanoma tumors with bacteriochlorophyll-serine-based photodynamic therapy. Photochem Photobiol 2001;73:257-66.

16. Seshadri M, Spernyak JA, Mazurchuk R, Camacho SH, Oseroff AR, Cheney RT, Bellnier DA. Tumor vascular response to photodynamic therapy and the antivascular agent 5,6-dimethylxanthenone-4-acetic acid: implications for combination therapy. Clin Cancer Res 2005;11:4241-50.

17. Yang M, Baranov E, Jiang P, Sun FX, Li XM, Li L, Hasegawa S, Bouvet M, Al-Tuwaijri M, Chishima T, Shimada H, Moossa AR, et al. Whole-body optical imaging of green fluorescent protein-expressing tumors and metastases. Proc Natl Acad Sci U S A 2000;97:1206-11.

18. Hoffman RM. The multiple uses of fluorescent proteins to visualize cancer in vivo. Nat Rev Cancer 2005;5:796-806.

19. Ntziachristos V. Fluorescence molecular imaging. Annu Rev Biomed Eng 2006;8:1-33.

20. Nguyen TH, Oberholzer J, Birraux J, Majno P, Morel P, Trono D. Highly efficient lentiviral vector-mediated transduction of nondividing, fully reimplantable primary hepatocytes. Mol Ther 2002;6:199-209.

21. Pogue BW, Gibbs SL, Chen B, Savellano M. Fluorescence imaging in vivo: raster scanned point-source imaging provides more accurate quantification than broad beam geometries. Technol Cancer Res Treat 2004;3:15-21.

22. Matsushita S, Chuang VT, Kanazawa M, Tanase S, Kawai K, Maruyama T, Suenaga A, Otagiri M. Recombinant human serum albumin dimer has high blood circulation activity and low vascular permeability in comparison with native human serum albumin. Pharm Res 2006;23:882-91.

23. Chen B, Pogue BW, Goodwin IA, O'Hara JA, Wilmot CM, Hutchins JE, Hoopes PJ, Hasan T. Blood flow dynamics after photodynamic therapy with verteporfin in the RIF-1 tumor. Radiat Res 2003;160:452-9.

24. Kurohane K, Tominaga A, Sato K, North JR, Namba Y, Oku N. Photodynamic therapy targeted to tumor-induced angiogenic vessels. Cancer Lett 2001;167:49-56.

25. Koudinova NV, Pinthus JH, Brandis A, Brenner O, Bendel P, Ramon J, Eshhar Z, Scherz A, Salomon Y. Photodynamic therapy with Pd-Bacteriopheophorbide (TOOKAD): successful in vivo treatment of human prostatic small cell carcinoma xenografts. Int J Cancer 2003;104:782-9.

26. Fukumura D, Jain RK. Tumor microenvironment abnormalities: causes, consequences, and strategies to normalize. J Cell Biochem 2007;101:937-49.

27. Heldin CH, Rubin K, Pietras K, Ostman A. High interstitial fluid pressure - an obstacle in cancer therapy. Nat Rev Cancer 2004;4:806-13.

28. Rofstad EK, Tunheim SH, Mathiesen B, Graff BA, Halsor EF, Nilsen K, Galappathi K. Pulmonary and lymph node metastasis is associated with primary tumor interstitial fluid pressure in human melanoma xenografts. Cancer Res 2002;62:661-4.

29. Boucher Y, Jain RK. Microvascular pressure is the principal driving force for interstitial hypertension in solid tumors: implications for vascular collapse. Cancer Res 1992;52:5110-4.

30. Fingar VH, Wieman TJ, Doak KW. Changes in tumor interstitial pressure induced by photodynamic therapy. Photochem Photobiol 1991;53:763-8.

31. Leunig M, Goetz AE, Gamarra F, Zetterer G, Messmer K, Jain RK. Photodynamic therapy-induced alterations in interstitial fluid pressure, volume and water content of an amelanotic melanoma in the hamster. Br J Cancer 1994;69:101-3.

32. Chen B, He C, de Witte P, Hoopes PJ, Hasan T, Pogue BW. Vascular targeting in photodynamic therapy. In: Hamblin MR. Advances in Photodynamic Therapy: Basic, Translational and Clinicaled. Norwood, MA: Artech House, Inc, 2008 (in press).

33. Snyder JW, Greco WR, Bellnier DA, Vaughan L, Henderson BW. Photodynamic therapy: a means to enhanced drug delivery to tumors. Cancer Res 2003;63:8126-31.

34. Debefve E, Pegaz B, Ballini JP, Konan YN, van den Bergh H. Combination therapy using aspirin-enhanced photodynamic selective drug delivery. Vascul Pharmacol 2007;46:171-80.

35. Ferrario A, von Tiehl KF, Rucker N, Schwarz MA, Gill PS, Gomer CJ. Antiangiogenic treatment enhances photodynamic therapy responsiveness in a mouse mammary carcinoma. Cancer Res 2000;60:4066-9.

36. Solban N, Selbo PK, Sinha AK, Chang SK, Hasan T. Mechanistic investigation and implications of photodynamic therapy induction of vascular endothelial growth factor in prostate cancer. Cancer Res 2006;66:5633-40.

37. Ferrario A, Von Tiehl K, Wong S, Luna M, Gomer CJ. Cyclooxygenase-2 inhibitor treatment enhances photodynamic therapy-mediated tumor response. Cancer Res 2002;62:3956-61.

38. Hendrickx N, Dewaele M, Buytaert E, Marsboom G, Janssens S, Van Boven M, Vandenheede JR, de Witte P, Agostinis P. Targeted inhibition of p38alpha MAPK suppresses

tumor-associated endothelial cell migration in response to hypericin-based photodynamic therapy. Biochem Biophys Res Commun 2005;337:928-35.

39. Ferrario A, Gomer CJ. Avastin enhances photodynamic therapy treatment of Kaposi's sarcoma in a mouse tumor model. J Environ Pathol Toxicol Oncol 2006;25:251-9.

40. Kosharskyy B, Solban N, Chang SK, Rizvi I, Chang Y, Hasan T. A mechanism-based combination therapy reduces local tumor growth and metastasis in an orthotopic model of prostate cancer. Cancer Res 2006;66:10953-8.

41. Li X, Zhao X, Fang Y, Jiang X, Duong T, Fan C, Huang CC, Kain SR. Generation of destabilized green fluorescent protein as a transcription reporter. J Biol Chem 1998;273:34970-5.

42. Vordermark D, Shibata T, Brown JM. Green fluorescent protein is a suitable reporter of tumor hypoxia despite an oxygen requirement for chromophore formation. Neoplasia 2001;3:527-34.

Legend

Figure 1. *In vivo* fluorescence images of the TRITC-albumin extravasation and tumor EGFP fluorescence. The EGFP-MatLyLu tumors were illuminated with 25 or 50 J/cm^2 light at 15 min after i.v. injection of 0.25 mg/kg dose of verteporfin. Immediately after treatment, tumor-bearing animals were i.v. injected with 20 mg/kg TRITC-albumin and imaged at different time after injection with a whole-body fluorescence imaging system as described in the Materials and Methods. Control tumors received no treatment. The images shown are the merged image of TRITC (red) and GFP (green) fluorescence images.

Figure 2. *In vivo* fluorescence image analysis showing *(a)* changes of the TRITC-albumin fluorescence intensity in tumor tissues, *(b)* changes of the TRITC-albumin fluorescence intensity in tumor-adjacent tissues, and *(c)* changes of tumor EGFP fluorescence intensity after treatment. The EGFP-MatLyLu tumors were treated with vascular-targeting PDT and imaged with a whole-body fluorescence imaging system. The TRITC and EGFP fluorescence intensities were measured in a circular ROI with 2.5 mm in diameter placed over the tumor or tumor-adjacent area on the fluorescence images. The fluorescence intensity values after treatment in each animal were normalized to their own pretreatment values, which are displayed as 100% at 0 time point. Each group included 3 or 4 animals. Error bars represent the standard deviation.

Figure 3. *In vivo* fluorescence image analysis showing the TRITC-albumin accumulation in relation to tumor EGFP fluorescence intensity. The 4 hour-time-point images from Figure 1 were analyzed and shown here. A 17-mm line was drawn through the tumor tissue on each fluorescence image. Both TRITC-albumin and tumor EGFP fluorescence intensities were measured alone the line and shown in the figure. The dashed line indicates the boundary of the tumor tissue. Note the opposite pattern between tumor TRITC-albumin accumulation and tumor EGFP fluorescence intensity profiles.

Figure 4. *Ex vivo* fluorescence microscopic images showing the distribution of TRITC-albumin in relation to the functional blood vessels highlighted by Hoechst dye staining. The EGFP-MatLyLu tumors were treated with 50 J/cm^2 light at 15 min after i.v. injection of 0.25 mg/kg dose of verteporfin. Control tumors received no treatment. Immediately after treatment, tumor-bearing animals were i.v. injected with 20 mg/kg TRITC-albumin. Animals were euthanized at 1, 4 or 24 hours after injection of the TRITC-albumin. Hoechst dye (20 mg/kg) was i.v. injected at 1 minute before euthanizing the animal. Frozen tumor sections from tissue samples were first imaged for the Hoechst and the same fields were then imaged for the TRITC-albumin fluorescence. All images shown include the tumor periphery. Bars = 100um.

Figure 5. *In vivo* tumor EGFP fluorescence images showing tumor response to the vascular-targeting PDT with verteporfin. The EGFP-MatLyLu tumors were treated with 25 or 50 J/cm^2 light at 15 min after i.v. injection of 0.25 mg/kg dose of verteporfin. Tumor EGFP fluorescence was imaged daily for up to 9 days after treatment with a whole-body fluorescence imaging

system as described in the Materials and Methods. Images at Day 0 were taken right before treatment. Control tumors received no treatment. Scale bar = 10 mm.

Figure 6. Tumor volume changes after the vascular-targeting PDT with verteporfin. The EGFP-MatLyLu tumors were treated with 25 or 50 J/cm^2 light at 15 min after i.v. injection of 0.25 mg/kg dose of verteporfin. Control tumors received no treatment. Tumor volume at Day 0 represented the starting volume right before the treatment.

Figure 7. H&E staining images showing the existence of viable tumor cells at tumor periphery after the vascular-targeting PDT with verteporfin. The EGFP-MatLyLu tumors were treated with 50 J/cm^2 light at 15 min after i.v. injection of 0.25 mg/kg dose of verteporfin. H&E staining of tumor sections taken at 48 hours after treatment showed wide spread tumor cell death and vascular damage. But a small number of viable tumor cells were detected at the tumor periphery. Part of the image on the left, highlighted in the box, is shown at a higher magnification on the right. The letters V and D indicate the viable tumor area and the dead tumor area, respectively. Bars = 100 um.

Figure 1

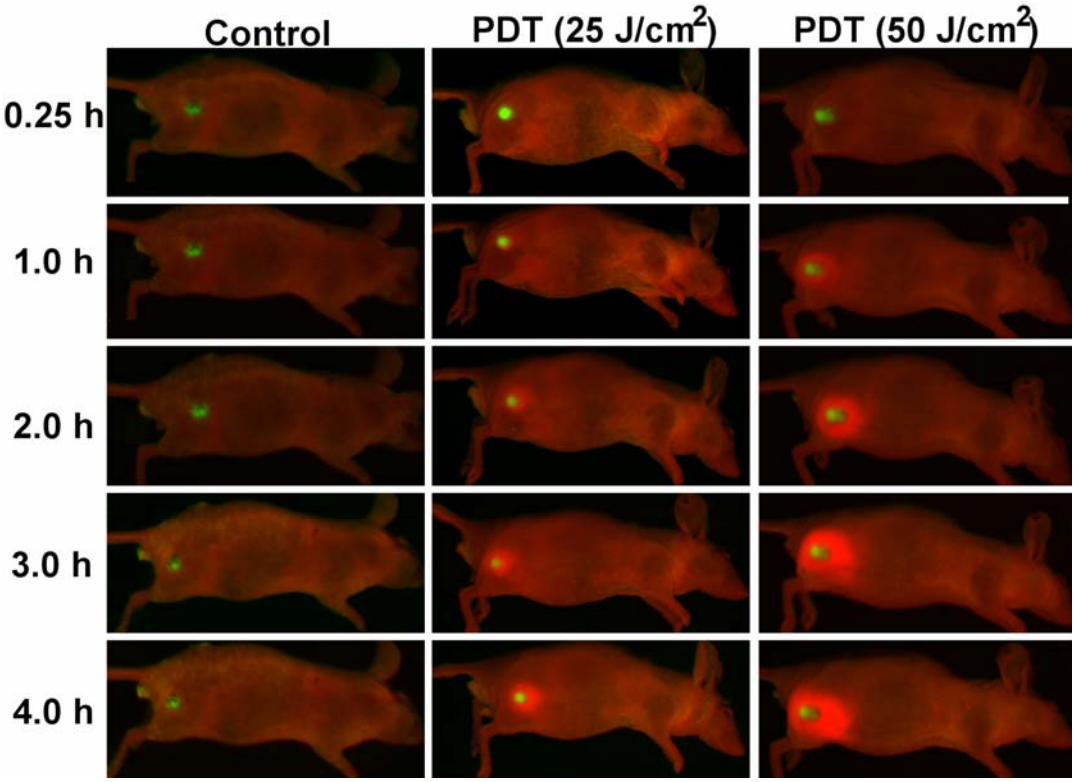

Figure 2

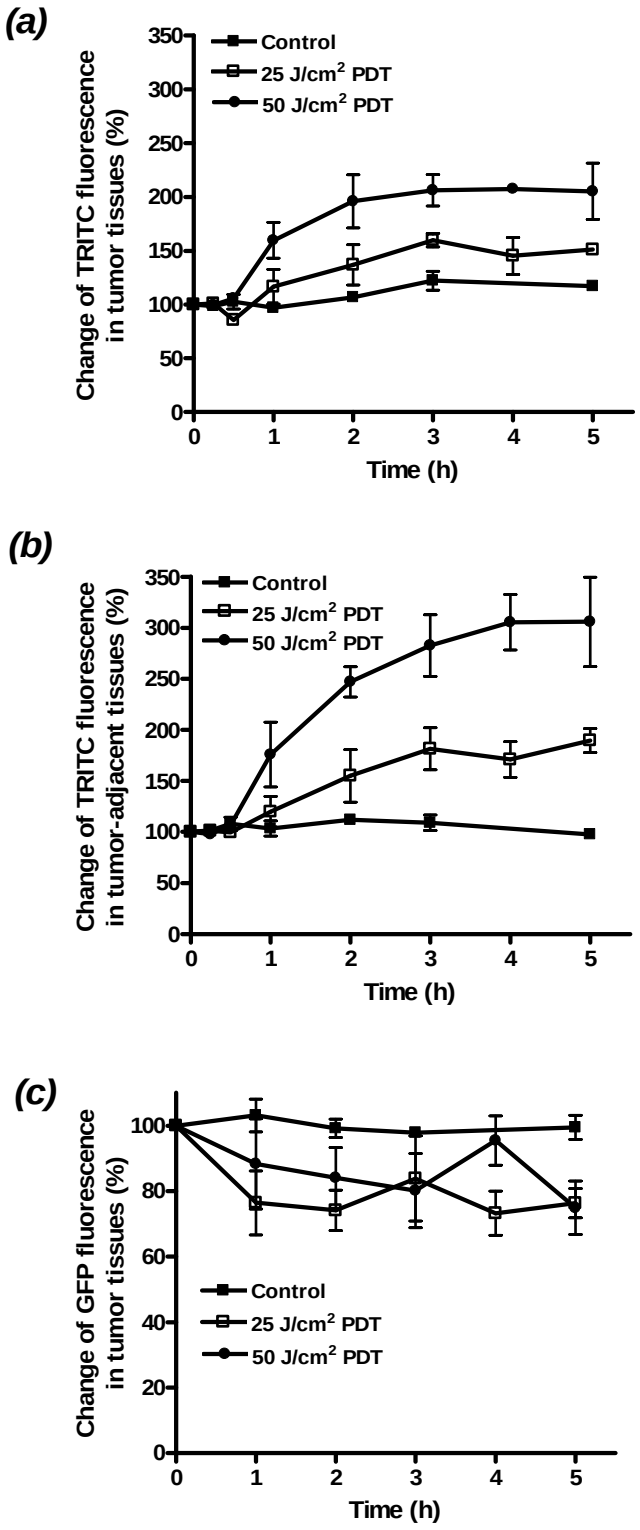
(a)
Change of TRITC fluorescence in tumor tissues (%)
Control
25 J/cm2 PDT
50 J/cm2 PDT
Time (h)
(b)
Change of TRITC fluorescence in tumor-adjacent tissues (%)
Control
25 J/cm2 PDT
50 J/cm2 PDT
Time (h)
(c)
Change of GFP fluorescence in tumor tissues (%)
Control
25 J/cm2 PDT
50 J/cm2 PDT
Time (h)

Figure 3

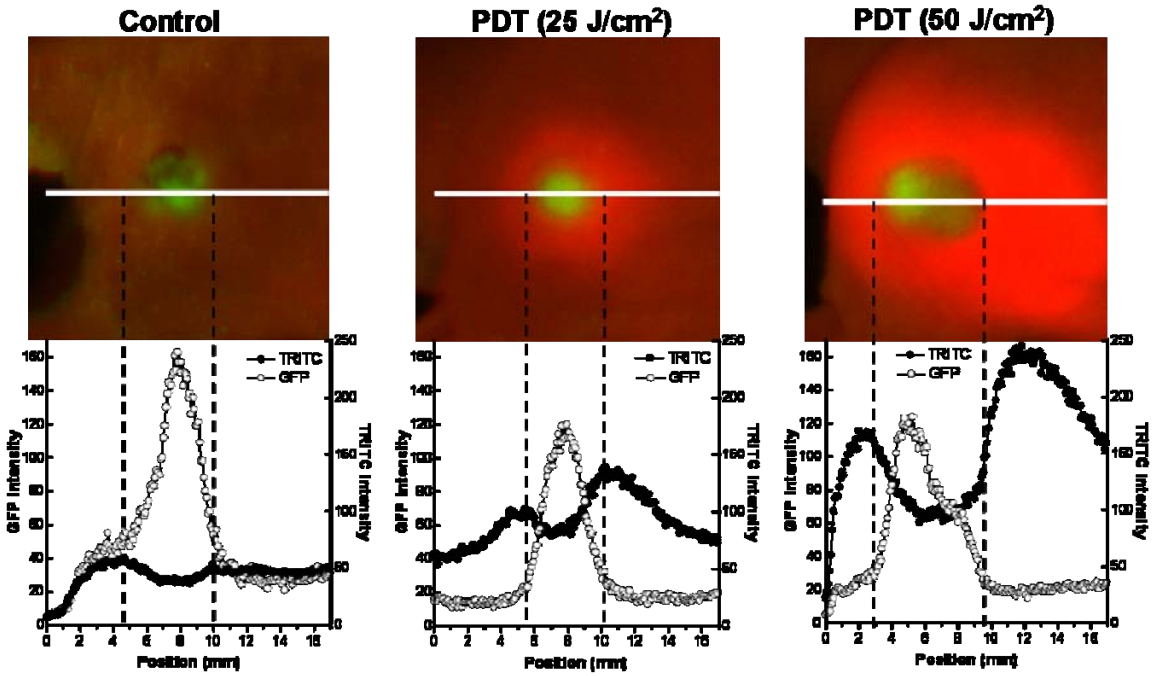
Control
PDT (25 J/cm2)
PDT (50 J/cm2)
TRITC
GFP
GFP Intensity
TRITC Intensity
Position (mm)

Figure 4

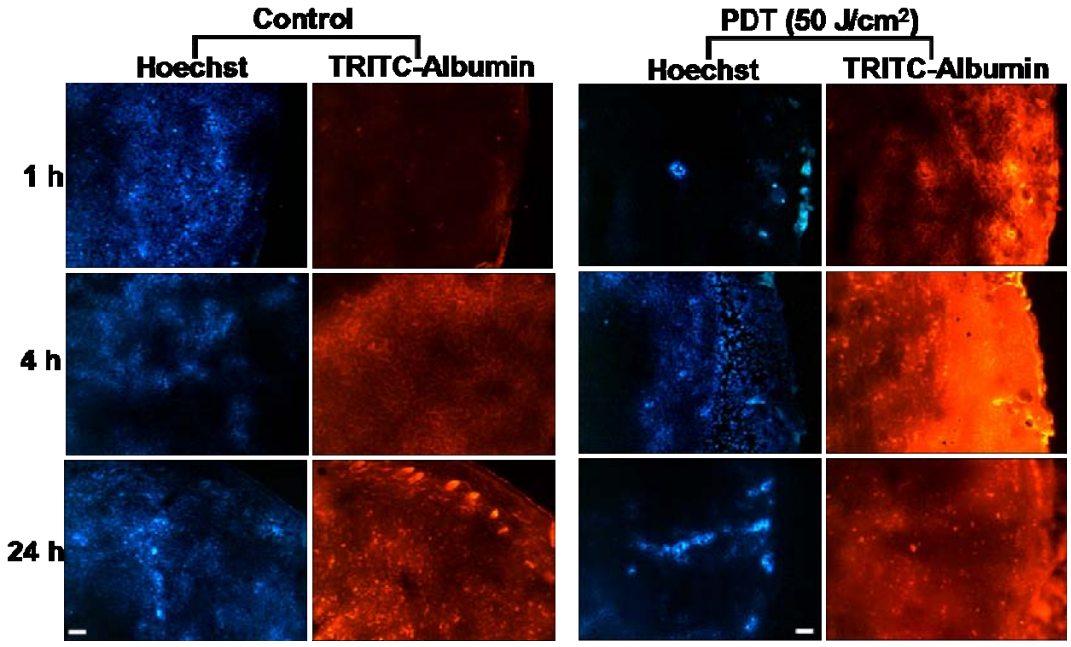
Control
PDT (50 J/cm²)
Hoechst
TRITC-Albumin
Hoechst
TRITC-Albumin
1 h
4 h
24 h

Figure 5

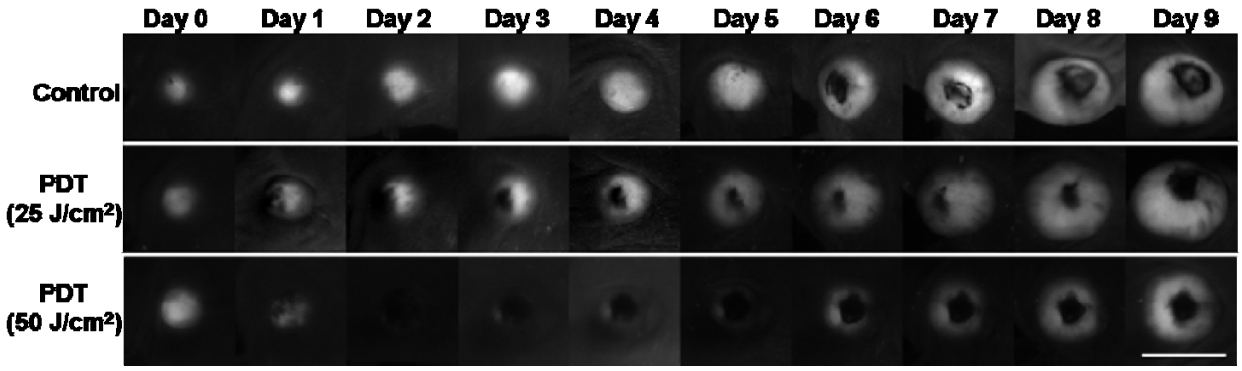
Day 0
Day 1
Day 2
Day 3
Day 4
Day 5
Day 6
Day 7
Day 8
Day 9
Control
PDT
(25 J/cm²)
PDT
(50 J/cm²)

Figure 6

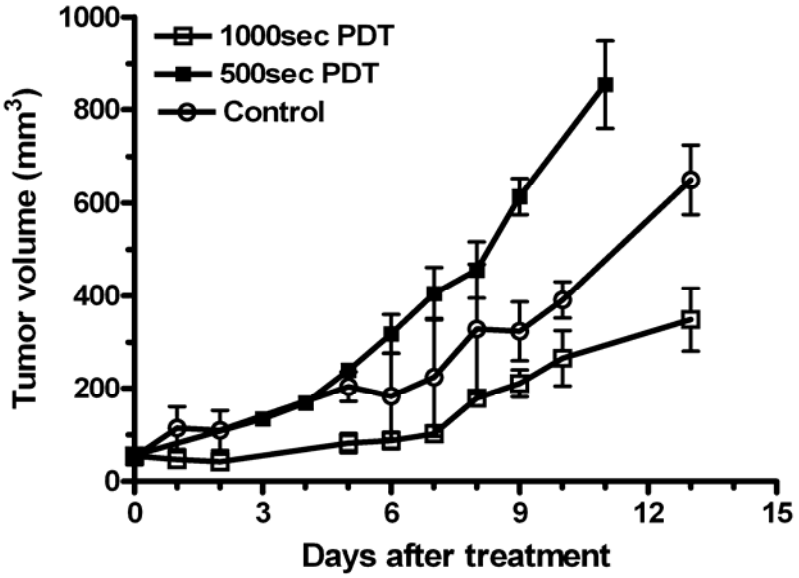
1000sec PDT
500sec PDT
Control
Tumor volume (mm3)
1000
800
600
400
200
0
0
3
6
9
12
15
Days after treatment

Figure 7

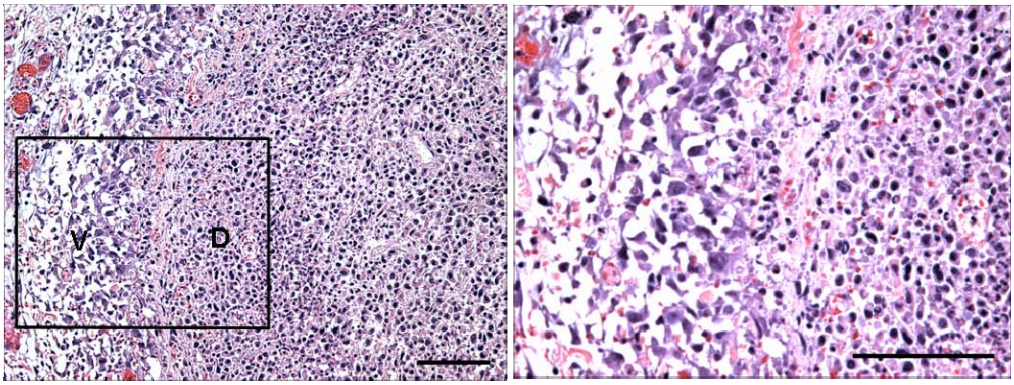

Vascular Targeting in Photodynamic Therapy

Bin Chen[1,2 *], Chong He[1], Peter de Witte[3], P. Jack Hoopes[4,5], Tayyaba Hasan[6], Brian W. Pogue[5,6]

[1]Department of Pharmaceutical Sciences, Philadelphia College of Pharmacy, University of the Sciences in Philadelphia, Philadelphia, PA 19104; [2]Department of Radiation Oncology, University of Pennsylvania, Philadelphia, PA 19104; [3]Laboratory of Pharmaceutical Biology and Phytopharmacology, Faculty of Pharmaceutical Sciences, Catholic University Leuven, B-3000 Leuven, Belgium; [4]Department of Surgery, Dartmouth Medical School, Lebanon, NH 03756; [5]Thayer School of Engineering, Dartmouth College, Hanover, NH 03755; [6]Wellman Center for Photomedicines, Massachusetts General Hospital, Harvard Medical School, Boston, MA 02114.

***Corresponding to:** Bin Chen, Ph.D., Department of Pharmaceutical Sciences, Philadelphia College of Pharmacy, University of the Sciences in Philadelphia, 600 South 43rd Street, Philadelphia, PA 19104. Tel: 215-596-7481; Fax: 215-895-1161; Email: b.chen@usip.edu.

Abstract

As a functional vascular system is vital for the survival and growth of tumor tissues, selective targeting of tumor vasculature is being perused actively as a treatment for cancer. Photodynamic therapy (PDT), depending on *in situ* generation of reactive oxygen species through photochemical reactions, has been used clinically in the management of cancer and non-cancer diseases. Although vascular damage contributes significantly to the antitumor effect of conventional PDT, this vascular effect can be substantially enhanced by novel vascular-targeting PDT regimen. Different from conventional PDT, vascular-targeting PDT solely relies on vascular photosensitization as a result of site-directed photosensitizer delivery. At the time of irradiation, there is little photosensitizer accumulation in the tumor cellular compartment. According to how photosensitizer is preferentially delivered to the tumor vasculature, photodynamic vascular targeting therapy can be divided into passive or active vascular-targeting PDT. Passive vascular-targeting PDT, primarily based on high plasma photosensitizer concentration at a short time after injection, has been successfully translated into clinical applications and research on active vascular-targeting PDT by taking advantage of novel tumor vascular markers and targeted drug delivery systems is emerging. Vascular-targeting PDT induces vascular shutdown through poorly characterized mechanisms, which kill tumor cells via tumor anoxia and ischemia. However, peripheral tumor vessels are often found less responsive to the vascular-targeting PDT than central blood vessels. The survival of some peripheral tumor vessels as well as their surrounding tumor cells after the non-curative vascular photosensitization activates cell growth and surviving pathways, creating a favorable tumor microenvironment to stimulate tumor recurrence and even metastasis. Future efforts should focus on further understanding the mechanisms of vascular photosensitization and what accounts for the existence of peripheral functional vessels after vascular-targeting PDT so that more curative treatments can be delivered. It is also important to understand the molecular machinery that tumor endothelial cells and tumor cells possess in order to survive PDT-induced tissue hypoxia. Therefore, we can apply rational-based combination therapy to specifically inhibit such survival signals for an enhanced therapeutic effect.

1. **Introduction**

Photodynamic therapy (PDT) induces tumor destruction through a photochemical reaction involving a photosensitizer, light of a specific wavelength matching the absorption wavelength of the photosensitizer, and the molecular oxygen [1]. Singlet oxygen, a product of this photochemical reaction, is mainly responsible for the biological effects of PDT by causing oxidative damages to the target cells and tissues [2]. After several decades' effort, PDT has become an established modality in medicine. Currently, PDT is being offered for the treatment of various types of cancer including lung, skin, gastrointestinal tract, head and neck and urological cancers [3] and non-cancer diseases such as age-related macular degeneration (AMD), atherosclerosis, viral or bacterial infections [4].

The mechanism of PDT in cancer treatment is complicated and evolves as our understanding of cancer biology and pharmacology progresses. It is now clear that PDT can either directly kill tumor cells or indirectly induce tumor cell death as a result of direct damage to tumor stroma [5]. Adequate and simultaneous deposition of a photosensitizer, light and oxygen molecules in tumor cells will cause tumor cell death. However, this direct photocytotoxicity is often limited (generally less than 1-log) in tumor cell killing likely due to inadequate supply of photosensitizers, light and/or oxygen in tumor tissues [6]. Tumor vasculature is an important target of PDT and this indirect tumor targeting mechanism is mainly responsible for the acute decrease of tumor burden after PDT with most photosensitizers [5]. Furthermore, PDT-induced inflammation as well as direct photosensitizing effects on immune cells may activate body immune system and lead to the generation of tumor-specific immunity, which is important for maintaining long-term tumor control [7].

For most photosensitizers, vascular damage is the predominant PDT effect and primarily responsible for the final treatment outcome [5]. Because of this, vascular-targeting PDT has been developed to further potentiate vascular damage. In this chapter, we will focus on vascular targeting in PDT. This targeting mechanism has led to so far the most successful application of PDT and is showing great promise in cancer treatment as well. We will discuss photodynamic vascular targeting principle, mechanisms, challenges and strategies to enhance its therapeutic outcome.

2. Tumor vascular targeting

It is well-known that solid tumors can not grow larger than about 1 mm^3 without developing a vascular network [8]. This is because, similar to normal tissues, tumor tissues require a functional vascular system for the delivery of nutrients and the removal of metabolic wastes. To sustain tumor growth, tumor tissues need to depend upon existing host vessels as well as develop new blood vessels for blood supply. Compared to the normal vasculature, tumor blood vessels exhibit significant abnormalities in vessel architecture (e.g. tortuousity, dilatation, irregular branching and lack of pericyte and basement membrane coverage) and function (e.g. stagnant blood flow, increased vascular permeability) [9]. Although the mechanisms leading to tumor vessel structural and functional abnormalities are not well understood, the imbalance between pro- and anti-angiogenic factors and mechanical compression generated by high tumor interstitial pressure and proliferating tumor cells have been suggested to be the major contributing factors [9]. The differences between tumor *versus* normal vasculature in the vessel molecular signature, structure and function provide the basis for selective tumor vascular targeting.

Vascular-targeting therapy can be divided into antiangiogenic therapy that inhibits the formation of new vessels and vascular-disrupting therapy that targets the existing blood vessels

[10]. The overall goal of tumor vascular targeting therapy is to selectively disrupt or modulate tumor vascular function for the therapeutic purposes without affecting much normal tissue functions. This modality can be used alone as monotherapy, but more often it is used in combination with other therapies in cancer treatment. Tumor vascular targeting strategy has several apparent advantages over the conventional tumor cellular targeting approach [8, 11]. First of all, vascular targets are readily accessible to the therapeutic agents delivered intravenously whereas tumor cellular targets are typically difficult to reach due to the existence of various physiological barriers. Secondly, vascular targeting is highly efficient and potent in tumor cell killing because, unlike tumor cell-targeted therapies, not all the endothelial cells are necessary to be targeted to disrupt tumor vascular function. Instead, damage to a single endothelial cell or a portion of blood vessel may induce catastrophic effect on tumor perfusion, resulting in killing thousands of tumor cells that are dependent upon that vessel for blood supply. Thirdly, because endothelial cells are generally considered to be more genetically stable than tumor cells, the risk of acquiring drug resistance is usually low. These advantages render tumor vascular targeting a promising approach in current cancer therapy.

3. Principle of photodynamic vascular targeting

Photodynamic vascular targeting is based on site-directed delivery of photosensitizing agents to the vascular system followed by light irradiation to induce site-specific vascular photosensitizing effects. Since vasculature-directed photosensitizer delivery can be achieved by passive or active means, photodynamic vascular targeting can be further divided into passive or active targeting approach [5]. The passive vasculature-directed photosensitizer delivery is primarily based on the innate photosensitizer pharmacokinetic property that plasma drug level is often high shortly after intravenous administration of a photosensitizer (Figure 1 & 2). This time period when photosensitizer is mainly localized inside the vasculature provides a temporal window for the passive vascular targeting. Although the exact location of this temporal window is largely dependent on the plasma kinetics of individual photosensitizer, for most photosensitizers it typically occurs within 60 minutes after injection.

By contrast, active vascular-targeting PDT seeks to achieve vasculature-directed drug delivery by altering photosensitizer pharmacokinetic property through drug structure modification or drug formulation into a targeted delivery system [5]. A targeting moiety that has a high affinity to endothelial cell markers (e.g. integrins, VEGF receptors, tumor endothelial markers) or vessel supporting structures (e.g. fibronectin with ED-B domain) is often used in the photosensitizer modification. The resulting photosensitizer conjugates are expected to be selectively accumulated in the targeted blood vessels, leading to a site-specific photosensitization upon light activation.

4. Current status of photodynamic vascular targeting

Passive vascular-targeting PDT provides an effective way of targeting blood vessels and has been successfully translated into clinical application for diseases characterized by the over-proliferation of blood vessels. Based on this mechanism, verteporfin is currently being used for the treatment of age-related macular degeneration (AMD) and more photosensitizers such as tin ethyletiopurpurin (SnET2, Purlytin) and lutetium texaphyrin (Lu-Tex, Optrin) are under clinical trials for AMD. Quite a few photosensitizers have also been evaluated for cancer treatment based on this passive targeting mechanism [5]. Among these photosensitizes, Tookad is at the forefront in the development pipeline. Currently, Tookad is in a Phase I/II clinical trial for locally

recurrent prostate cancer after radiation therapy [12]. Although limited in the number of studies, active vascular-targeting PDT is being pursued actively for the treatment of cancer and non-cancer diseases. Promising results have been obtained from several studies of conjugating photosensitizers to the blood vessel-homing peptides [13-17].

5. Mechanisms of photodynamic vascular targeting

Photodynamic vascular targeting therapy has been shown to produce reactive oxygen species intravascularly, in particular singlet oxygen, which are believed to be mainly responsible for the subsequent vessel structural and functional alterations [18]. The ultimate goal of vascular-targeting PDT in cancer therapy is to obtain maximal tumor cell killing by inducing tumor vascular shutdown. The mechanism of PDT-induced vascular shutdown is complicated because it likely involves multiple targets in the blood cells and blood vessels, which are interweaved in complex cascades of events. Intravital fluorescence microscopic study demonstrates that microcirculation dysfunction after vascular-targeting PDT is induced by at least two vascular events, vessel occlusion induced by thrombus formation and vessel constriction/collapse caused by mechanic compression and vasoactive substances (Figure 2A, 2B).

Thrombus formation can be induced by photosensitizing damage to either blood cells or endothelial cells. It has been shown that PDT can cause platelet aggregation and thrombus formation by direct damage to the platelet and red blood cell membranes [19, 20]. Damage to the platelets may further stimulate the release of thromboxane, a vasoactive substance with potent vessel constriction and thrombus formation effects [21]. More often, PDT-induced damage to the blood cells is coupled with damage to the endothelial cells, which might explain why blood cell aggregation is often observed starting from the vessel wall. Since endothelium serves as an interface between blood and underneath tissue, loss of endothelial barrier as a result of vascular photosensitization exposes tissue extracellular matrix to the circulation, which activates platelets and polymorphonuclear leukocytes and induces blood cell adherence to the damaged endothelial cells. Thromboxane release as a result of platelet activation has been shown to contribute significantly to vessel constriction and thrombus formation, which can be inhibited by thromboxane inhibitors aspirin and indomethacin [22] or platelet depletion [21]. Endothelial cells also influence blood clotting balance by releasing von Willebrand factor that facilitates thrombus formation [23] and prostacyclin that inhibits thrombus formation and dilates blood vessels [24]. The net effect likely favors clot formation at least at early stage after vascular photosensitization. Blood clots formed inside vessel lumen cause obstruction to blood flow. However, blood vessels may resume perfusion because not all the clots are stable and some of them can be dissolved and dislodged possibly by body anticoagulants. Only the stable thrombi will finally occlude blood vessels and shutdown vascular function. Inhibition of thrombus formation by heparin has been shown to delay PDT-induced blood flow stasis [25]. But it is not able to completely inhibit blood flow decrease, suggesting that thrombus formation is only partially responsible for the vascular damage induced by PDT.

As a spontaneous response to blood vessel damages, vessel constriction is often observed after vascular photosensitization, which also contributes to PDT-induced blood flow stasis. Vessel constriction can be caused by the release of vasoactive substances such as thromboxane and leukotrienes [26]. However, a strong inducer of vessel constriction and even collapse in tumor tissues comes from the increase of interstitial fluid pressure [9]. It is well-established that tumor tissues generally have higher tissue interstitial pressure than the normal tissues because of leaky tumor blood vessels. The mechanic compression generated by high tumor interstitial

pressure can collapse tumor blood vessel even without treatment and this is one of the mechanisms involved in acute hypoxia development in tumor tissues [27]. Such vessel compression/collapse effects are aggravated by PDT because PDT is able to cause vascular barrier disruption and therefore further increase tumor interstitial pressure [28, 29].

Since endothelial cells play a critical role in maintaining vascular barrier and perfusion functions, it is important to study how endothelial cells respond to photosensitization at cellular and molecular levels. Studies with different photosensitizers have shown that photosensitization of endothelial cells induces rapid microtubule depolymerization followed by stress fiber actin formation and cell rounding [30, 31]. Although it is not clear how microtubule damage results in endothelial cell shape change, microtubule depolymerization is believed to initiate subsequent vessel functional changes because endothelial cell barrier function is dependent on endothelial cell morphology regulated by cell cytoskeleton. Indeed, photosensitization-induced endothelial cell shape change has been shown to be correlated to the permeability increase [31]. Increase in cytosol calcium concentration has been suggested to be the cause of microtubule depolymerization [30]. However, direct photosensitizing damage to the microtubules can not be ruled out. Nevertheless, vascular permeability increase has been observed in both animal and human studies shortly after PDT [26, 32], suggesting that this is an early event following endothelial cell damage. The disruption of vascular barrier function will trigger the subsequent thrombus formation and vessel compression as described above.

The molecular mechanism involved in endothelial photosensitization is poorly studied. There are reports showing that photosensitization activates nuclear transcriptor NF-κB in endothelial cells through a reactive oxygen species-mediated mechanism [33, 34]. Since NF-κB is major regulator of inflammatory and immune reactions, its activation in endothelial cells plays an important role in vascular photosensitization-induced tumor destruction. Paradoxically, NF-κB activation can cause both tumor inhibition and stimulation [35]. Tumor inhibition is related to its role in enhancing gene expression of cytokines (IL-6, TNF-α), adhesion molecules (intercellular adhesion molecule-1, vascular cell adhesion molecule-1) and possibly heat shock proteins [34, 36]. As a result, vascular photosensitization treatment is able to stimulate blood cells especially neutrophils adhesion to the endothelial cells, inducing vascular damages. On the other hand, tumor stimulation as a consequence of NF-κB activation is associated with the upregulation of cyclooxygenas-2 (COX-2), matrix metalloproteases (MMPs) and inhibitors of apoptosis [35]. Although there is no report demonstrating the upregulation of COX-2 and apoptosis inhibitors in endothelial cells, which has been shown in tumor cells, the induction of MMP-9 expression has been confirmed in endothelial cells after PDT, suggesting a role of NF-κB activation in endothelial resistance to photosensitization [35]. Interestingly, pretreatment of endothelial cells with photosensitization or other oxidative stress has been shown to induce cell adaptation, resulting in the upregulation of heat shock protein and anti-oxidation enzymes through the p38 MARK pathway. This cellular adaptation to the oxidative stressors indeed renders endothelial cells' resistance to the subsequent treatment [37].

6. Therapeutic challenges of photodynamic vascular targeting

Although vascular-targeting PDT is able to induce extensive tumor vascular shutdown and, consequently, tumor cell death, functional blood vessels are typically detected at tumor peripheral areas following non-curative treatments. The existence of these functional blood vessels can lead to tumor recurrence, which is often observed starting from the peripheral tumor area [38, 39]. Figure 2F shows representative tumor fluorescence images after verteporfin-PDT.

In this experiment, we used a lentivirus-transduced MatLyLu prostate tumor cell line that permanently expresses EGFP. The EGFP-MatLyLu tumors were imaged non-invasively for the EGFP fluorescence before and after PDT by using a whole-body fluorescence imaging system. Because dead EGFP-MatLyLu tumor cells were not able to produce EGFP, dead tumor tissues would appear as dark areas and only viable tumor tissues could be visible on tumor EGFP fluorescence images. Control tumors grew rapidly and generally exhibited central necrosis when tumor reached about 8-10 mm in diameter. The 50 J/cm^2 PDT was effective in eradicating tumor tissue and little EGFP fluorescence was detected by 2 days after PDT. However, small EGFP fluorescent spots, indicating the existence of viable tumor cells, were detected at tumor edges several days after treatment. Peripheral viable tumor tissues were found growing rapidly, leading to tumor recurrence.

It is still not clear why tumor peripheral and central blood vessels react differently to the vascular photosensitization. It is hypothesized that such a variation in vascular response is likely related to the differences in tumor interstitial pressure and the structure of blood vessels in tumor central *versus* peripheral areas. Because the tumor central area generally has a higher interstitial pressure than the peripheral area, central blood vessels are more likely to collapse than the peripheral vessels as a result of higher mechanic compression [40, 41]. Moreover, peripheral tumor blood vessels are generally found to be larger and have more vessel supporting structures such as pericytes than the central tumor vessels (Figure 2E). Collectively, less tumor interstitial pressure together with more vessel supporting structures might make peripheral tumor vessels more resistant to the vessel compression/collapse imposed by PDT-induced tumor interstitial pressure elevation. Survival of these peripheral blood vessels after vascular photosensitization provides a chance of survival to the tumor cells supported by these vessels.

To maintain tissue integrity and function, biological systems develop sets of well-balanced repairing and adaptive mechanisms to deal with various internal and external damages. Through complicated and often redundant signaling cascades, cells are able to survive nonfatal damages by stimulating cell growth, tissue angiogenesis and remodeling. Unfortunately, tumor endothelial and tumor cells can hijack these spontaneous responses to obtain their own survival after sub-curative treatments, leading to disease recurrence. As mentioned above, photosensitization activates p38 MAPK survival signaling in endothelial cells [37]. The activation of p38 MARK is able to further induce the upregulation of COX-2, which catalyzes the conversion of arachidonic acid to prostaglandins (PGs) [42, 43]. PGs, especially PGE_2, have been shown to enhance cell motility, adhesion and survival, and stimulate tumor angiogenesis by inducing VEGF release. Furthermore, elevated VEGF release can also be obtained via HIF-1-mediated signaling pathway activated by PDT-induced tissue hypoxia [44, 45]. Clearly through the activation of these self-repairing and surviving pathways, tumor endothelial and tumor cells actually create a favorable microenvironment to maintain their survival and growth. It is not unusual to observe that tumor cells after sub-curative PDT treatments are actually becoming more aggressive [45, 46]. In the end, non-curative treatments might unintentionally select a small population of cells that are good at manipulating normal physiological pathways to survive therapeutic stressors. Therefore, how to target cell survival signals and adaptation mechanisms represents a major therapeutic challenge for not only photodynamic vascular targeting, but also all other cancer therapies.

7. Strategies to enhance photodynamic vascular targeting

As combination therapy has been routinely used in cancer treatment, one approach of enhancing photodynamic vascular targeting efficacy is to combine it with other cancer therapies.

Combination therapies can be designed based on several different targeting principles. Targeting both tumor vascular and cellular compartments by combining photodynamic vascular targeting therapy with a cancer cell-targeted therapy has been demonstrated to be an effective strategy. For instance, more than additive antitumor effects have been obtained from most early studies exploring the combination of PDT and cancer chemotherapy [47, 48]. Recently, PDT itself has been studied for targeting tumor blood vessels or tumor cells and enhanced therapeutic effects have been reported from studies with combined PDT regimens that target both tumor compartments. These dual targeting PDT treatments include PDT using a vascular-targeting photosensitizer Photofrin in combination with PDT using a cellular-targeting photosensitizer 5-aminolevulinic acid (5-ALA) [49], PDT regimen based on photosensitizer dose fractionation protocol so that light can be delivered when photosensitizer has been deposited in both vascular and cellular compartments [50], and sequential combination of a cancer cell-targeted PDT followed by a blood vessel-targeted PDT [38].

Although the mechanisms responsible for such enhanced antitumor effects are still not clear, spatial cooperation in tumor cell killing between vascular-targeting PDT and cancer cell-targeted therapies possibly plays a role here. As mentioned above, vascular-targeting PDT is especially effective in inducing central tumor cell death. Cancer cell-targeted therapies however mainly kill peripheral PDT tumor cells because most anticancer agents including photosensitizers tend to accumulate more at the tumor periphery presumably because of better perfusion at tumor peripheral areas [51, 52]. Thus, cancer cell-targeted therapies may complement vascular-targeting PDT in reducing some peripheral tumor cells that are otherwise not able to be killed by vascular-targeting PDT. The other mechanism possibly involved in the therapeutic enhancement is that both conventional and vascular-targeting PDT treatments have been shown to improve drug delivery to tumor tissues as a result of PDT-induced vascular permeability increase [31, 53]. Interestingly, we have found that such an enhancement in tumor drug delivery caused by vascular-targeting PDT is actually more pronounced in the tumor peripheral area than in the tumor central area (not yet published observation). The overall increase of the anticancer agent in the tumor tissue, tumor peripheral areas in particular, after vascular-targeting PDT may also account for the improved antitumor effect.

The other important combination strategy is to target the surviving and repairing pathways which tumor endothelial cells as well as tumor cells depend on to maintain their survival after vascular-targeting PDT. An example in this case is the combination of vascular-targeting PDT with antiangiogenic therapy. PDT treatments have been found to stimulate angiogenesis and tumor growth by inducing VEGF upregulation [44, 45]. Depending on the photosensitizer, the type of tumor model and treatment conditions, the elevation of VEGF can be caused by hypoxia-induced HIF-1 activation [44], COX-2 overexpression [43, 54] and p38 MAPK activation [45]. Thus, combined treatments of PDT with VEGF antibody bevacizumab [55], antiangiogenic drug TNP-470 [56] or COX-2 inhibitor [54] have all been shown to enhance the therapeutic effects. As our understanding regarding tumor/endothelial cell adaptation to therapeutic stressors increases, more such rationale-designed combination regimens will be designed to target crucial cellular and molecular surviving pathways, leading to a synergistic treatment outcome.

8. Summary and conclusions

Vascular damage is the most important mechanism involved in PDT-mediated tumor eradication. Vascular-targeting PDT is designed to further strengthen this vascular photosensitization effect by site-directed delivery of photosensitizing agents to the vascular

targets. Being so far the most successful PDT regimen, vascular-targeting PDT has been used clinically in the management of AMD and is showing great promise in cancer treatment as well. However, spatial heterogeneity in the vascular response and tumor/endothelial cell adaptation to the oxidative and hypoxic stressors often result in tumor recurrence. Therefore, a combination therapy with modalities complementary to the vascular-targeting PDT in tumor cell killing or treatments targeting cell surviving and adaptive signaling pathways often shows better results than vascular-targeting PDT alone. These combination regimens should be further evaluated in the clinic. Equally important, we need to further understand the mechanism of vascular-targeting PDT at tissue, cellular and molecular levels. It is obvious that 100% tumor cure can be achieved in preclinical animal tumor models with photodynamic vascular targeting therapies. The question is whether it is possible to delivery such curative, rather than sub-curative, vascular-targeting PDT to the patients, and how?

Acknowledgement

This work was supported by Department of Defense (DOD) Prostate Cancer Research Grant W81XWH-06-1-0148. The authors would like to gratefully acknowledge QLT Inc. for providing verteporfin.

References

1. Dougherty, T. J., et al., "Photodynamic therapy," *J Natl Cancer Inst*, Vol. 90, 1998, pp. 889-905
2. Schmidt, R., "Photosensitized generation of singlet oxygen," *Photochem Photobiol*, Vol. 82, 2006, pp. 1161-1177
3. Dolmans, D. E., Fukumura, D., and Jain, R. K., "Photodynamic therapy for cancer," *Nat Rev Cancer*, Vol. 3, 2003, pp. 380-387
4. Detty, M. R., Gibson, S. L., and Wagner, S. J., "Current clinical and preclinical photosensitizers for use in photodynamic therapy," *J Med Chem*, Vol. 47, 2004, pp. 3897-3915
5. Chen, B., et al., "Vascular and cellular targeting for photodynamic therapy," *Crit Rev Eukaryot Gene Expr*, Vol. 16, 2006, pp. 279-305
6. Henderson, B. W., and Dougherty, T. J., "How does photodynamic therapy work?," *Photochem Photobiol*, Vol. 55, 1992, pp. 145-157
7. Canti, G., De Simone, A., and Korbelik, M., "Photodynamic therapy and the immune system in experimental oncology," *Photochem Photobiol Sci*, Vol. 1, 2002, pp. 79-80
8. Siemann, D. W., Chaplin, D. J., and Horsman, M. R., "Vascular-targeting therapies for treatment of malignant disease," *Cancer*, Vol. 100, 2004, pp. 2491-2499
9. Fukumura, D., and Jain, R. K., "Tumor microenvironment abnormalities: causes, consequences, and strategies to normalize," *J Cell Biochem*, Vol. 101, 2007, pp. 937-949
10. Siemann, D. W., et al., "Differentiation and definition of vascular-targeted therapies," *Clin Cancer Res*, Vol. 11, 2005, pp. 416-420
11. Thorpe, P. E., "Vascular targeting agents as cancer therapeutics," *Clin Cancer Res*, Vol. 10, 2004, pp. 415-427
12. Pinthus, J. H., et al., "Photodynamic therapy for urological malignancies: past to current approaches," *J Urol*, Vol. 175, 2006, pp. 1201-1207
13. Birchler, M., et al., "Selective targeting and photocoagulation of ocular angiogenesis mediated by a phage-derived human antibody fragment," *Nat Biotechnol*, Vol. 17, 1999, pp. 984-988
14. Tirand, L., et al., "A peptide competing with VEGF165 binding on neuropilin-1 mediates targeting of a chlorin-type photosensitizer and potentiates its photodynamic activity in human endothelial cells," *J Control Release*, Vol. 111, 2006, pp. 153-164
15. Ichikawa, K., et al., "Antiangiogenic photodynamic therapy (PDT) by using long-circulating liposomes modified with peptide specific to angiogenic vessels," *Biochim Biophys Acta*, Vol. 1669, 2005, pp. 69-74
16. Reddy, G. R., et al., "Vascular targeted nanoparticles for imaging and treatment of brain tumors," *Clin Cancer Res*, Vol. 12, 2006, pp. 6677-6686
17. Frochot, C., et al., "Interest of RGD-containing linear or cyclic peptide targeted tetraphenylchlorin as novel photosensitizers for selective photodynamic activity," *Bioorg Chem*, Vol. 35, 2007, pp. 205-220
18. Gross, S., et al., "Monitoring photodynamic therapy of solid tumors online by BOLD-contrast MRI," *Nat Med*, Vol. 9, 2003, pp. 1327-1331
19. Fingar, V. H., Wieman, T. J., and Haydon, P. S., "The effects of thrombocytopenia on vessel stasis and macromolecular leakage after photodynamic therapy using photofrin," *Photochem Photobiol*, Vol. 66, 1997, pp. 513-517

20. Ben-Hur, E., et al., "Photodynamic treatment of red blood cell concentrates for virus inactivation enhances red blood cell aggregation: protection with antioxidants," *Photochem Photobiol*, Vol. 66, 1997, pp. 509-512
21. Fingar, V. H., Wieman, T. J., and Doak, K. W., "Role of thromboxane and prostacyclin release on photodynamic therapy-induced tumor destruction," *Cancer Res*, Vol. 50, 1990, pp. 2599-2603
22. Reed, M. W., et al., "The microvascular effects of photodynamic therapy: evidence for a possible role of cyclooxygenase products," *Photochem Photobiol*, Vol. 50, 1989, pp. 419-423
23. Foster, T. H., et al., "Photosensitized release of von Willebrand factor from cultured human endothelial cells," *Cancer Res*, Vol. 51, 1991, pp. 3261-3266
24. Henderson, B. W., et al., "Effects of photodynamic treatment of platelets or endothelial cells in vitro on platelet aggregation," *Photochem Photobiol*, Vol. 56, 1992, pp. 513-521
25. Dolmans, D. E., et al., "Vascular accumulation of a novel photosensitizer, MV6401, causes selective thrombosis in tumor vessels after photodynamic therapy," *Cancer Res*, Vol. 62, 2002, pp. 2151-2156
26. Fingar, V. H., "Vascular effects of photodynamic therapy," *J Clin Laser Med Surg*, Vol. 14, 1996, pp. 323-328
27. Vaupel, P., and Mayer, A., "Hypoxia in cancer: significance and impact on clinical outcome," *Cancer Metastasis Rev*, Vol. 26, 2007, pp. 225-239
28. Fingar, V. H., Wieman, T. J., and Doak, K. W., "Changes in tumor interstitial pressure induced by photodynamic therapy," *Photochem Photobiol*, Vol. 53, 1991, pp. 763-768
29. Leunig, M., et al., "Photodynamic therapy-induced alterations in interstitial fluid pressure, volume and water content of an amelanotic melanoma in the hamster," *Br J Cancer*, Vol. 69, 1994, pp. 101-103
30. Sporn, L. A., and Foster, T. H., "Photofrin and light induces microtubule depolymerization in cultured human endothelial cells," *Cancer Res*, Vol. 52, 1992, pp. 3443-3448
31. Chen, B., et al., "Tumor vascular permeabilization by vascular-targeting photosensitization: effects, mechanism, and therapeutic implications," *Clin Cancer Res*, Vol. 12, 2006, pp. 917-923
32. Schmidt-Erfurth, U., et al., "Time course and morphology of vascular effects associated with photodynamic therapy," *Ophthalmology*, Vol. 112, 2005, pp. 2061-2069
33. Volanti, C., Matroule, J. Y., and Piette, J., "Involvement of oxidative stress in NF-kappaB activation in endothelial cells treated by photodynamic therapy," *Photochem Photobiol*, Vol. 75, 2002, pp. 36-45
34. Volanti, C., et al., "Downregulation of ICAM-1 and VCAM-1 expression in endothelial cells treated by photodynamic therapy," *Oncogene*, Vol. 23, 2004, pp. 8649-8658
35. Matroule, J. Y., Volanti, C., and Piette, J., "NF-kappaB in photodynamic therapy: discrepancies of a master regulator," *Photochem Photobiol*, Vol. 82, 2006, pp. 1241-1246
36. Korbelik, M., Sun, J., and Cecic, I., "Photodynamic therapy-induced cell surface expression and release of heat shock proteins: relevance for tumor response," *Cancer Res*, Vol. 65, 2005, pp. 1018-1026
37. Plaks, V., et al., "Homologous adaptation to oxidative stress induced by the photosensitized Pd-bacteriochlorophyll derivative (WST11) in cultured endothelial cells," *J Biol Chem*, Vol. 279, 2004, pp. 45713-45720

38. Chen, B., et al., "Combining vascular and cellular targeting regimens enhances the efficacy of photodynamic therapy," *Int J Radiat Oncol Biol Phys*, Vol. 61, 2005, pp. 1216-1226
39. Chen, B., Roskams, T., and de Witte, P. A., "Antivascular tumor eradication by hypericin-mediated photodynamic therapy," *Photochem Photobiol*, Vol. 76, 2002, pp. 509-513
40. Boucher, Y., and Jain, R. K., "Microvascular pressure is the principal driving force for interstitial hypertension in solid tumors: implications for vascular collapse," *Cancer Res*, Vol. 52, 1992, pp. 5110-5114
41. Rofstad, E. K., et al., "Pulmonary and lymph node metastasis is associated with primary tumor interstitial fluid pressure in human melanoma xenografts," *Cancer Res*, Vol. 62, 2002, pp. 661-664
42. Hendrickx, N., et al., "Up-regulation of cyclooxygenase-2 and apoptosis resistance by p38 MAPK in hypericin-mediated photodynamic therapy of human cancer cells," *J Biol Chem*, Vol. 278, 2003, pp. 52231-52239
43. Hendrickx, N., et al., "Targeted inhibition of p38alpha MAPK suppresses tumor-associated endothelial cell migration in response to hypericin-based photodynamic therapy," *Biochem Biophys Res Commun*, Vol. 337, 2005, pp. 928-935
44. Ferrario, A., et al., "Antiangiogenic treatment enhances photodynamic therapy responsiveness in a mouse mammary carcinoma," *Cancer Res*, Vol. 60, 2000, pp. 4066-4069
45. Solban, N., et al., "Mechanistic investigation and implications of photodynamic therapy induction of vascular endothelial growth factor in prostate cancer," *Cancer Res*, Vol. 66, 2006, pp. 5633-5640
46. Momma, T., et al., "Photodynamic therapy of orthotopic prostate cancer with benzoporphyrin derivative: local control and distant metastasis," *Cancer Res*, Vol. 58, 1998, pp. 5425-5431
47. Streckyte, G., et al., "Effects of photodynamic therapy in combination with Adriamycin," *Cancer Lett*, Vol. 146, 1999, pp. 73-86
48. Ma, L. W., et al., "Enhanced antitumour effect of photodynamic therapy by microtubule inhibitors," *Cancer Lett*, Vol. 109, 1996, pp. 129-139
49. Peng, Q., et al., "Antitumor effect of 5-aminolevulinic acid-mediated photodynamic therapy can be enhanced by the use of a low dose of photofrin in human tumor xenografts," *Cancer Res*, Vol. 61, 2001, pp. 5824-5832
50. Dolmans, D. E., et al., "Targeting tumor vasculature and cancer cells in orthotopic breast tumor by fractionated photosensitizer dosing photodynamic therapy," *Cancer Res*, Vol. 62, 2002, pp. 4289-4294
51. Jain, R. K., "Delivery of molecular medicine to solid tumors: lessons from in vivo imaging of gene expression and function," *J Control Release*, Vol. 74, 2001, pp. 7-25
52. Pogue, B. W., et al., "Analysis of sampling volume and tissue heterogeneity on the in vivo detection of fluorescence," *J Biomed Opt*, Vol. 10, 2005, pp. 41206
53. Snyder, J. W., et al., "Photodynamic therapy: a means to enhanced drug delivery to tumors," *Cancer Res*, Vol. 63, 2003, pp. 8126-8131
54. Ferrario, A., et al., "Cyclooxygenase-2 inhibitor treatment enhances photodynamic therapy-mediated tumor response," *Cancer Res*, Vol. 62, 2002, pp. 3956-3961

55. Ferrario, A., and Gomer, C. J., "Avastin enhances photodynamic therapy treatment of Kaposi's sarcoma in a mouse tumor model," *J Environ Pathol Toxicol Oncol*, Vol. 25, 2006, pp. 251-259
56. Kosharskyy, B., et al., "A mechanism-based combination therapy reduces local tumor growth and metastasis in an orthotopic model of prostate cancer," *Cancer Res*, Vol. 66, 2006, pp. 10953-10958

Legends

Figure 1. Photodynamic tumor vascular targeting with photosensitizer hypericin. Fluorescence image of hypericin (A) and the corresponding H&E staining photograph (B) demonstrate the intravascular localization of hypericin at 30 minutes after i.v. injection of 5 mg/kg dose of hypericin in the RIF-1 mouse tumor model. The letter v indicates blood vessels. Vascular-targeting PDT with hypericin, i.e. light treatment at 30 min after 5 mg/kg dose of hypericin injection, caused vascular shutdown in central tumor areas. However, some tumor peripheral blood vessels were still functional, as indicated by the presence of Hoechst dye fluorescence (C), which was injected 1 minute before euthanizing the animal. The corresponding H&E staining image (D) confirmed the vessel histology. The arrows indicate the functional blood vessels at the tumor periphery. Vascular-targeting PDT with hypericin, i.e. light treatment at 30 minutes after 1 mg/kg dose of hypericin injection, significantly inhibited the RIF tumor growth and its antitumor effect can be further enhanced by subcutaneous injection of antiangiogenic drug TNP-470 at a dose of 30 mg/kg once every two days. Each group included 8-10 animals.

Figure 2. Photodynamic tumor vascular targeting with photosensitizer verteporfin. (A) Intravital fluorescence microscopic images showing intravascular localization of verteporfin and thrombus formation after vascular-targeting PDT in the orthotopic MatLyLu rat prostate tumor. Rat blood cells were labeled with fluorescent dye Dil and injected (i.v.) to the animals to highlight blood vessels. The MatLyLu tumors were treated with 50 J/cm^2 light (690 nm, at 50 mW/cm^2) at 15 min after i.v. injection of 0.25 mg/kg verteporfin to target tumor blood vessels. The first image was taken right before light treatment showing the localization of verteporfin (red) in tumor blood vessels (green). Blood cell adherence and thrombus formation, indicated by arrows, were clearly visible after vascular-targeting PDT. (B) Intravital fluorescence microscopic imaging of vascular permeability increase and vessel compression after vascular-targeting PDT with verteporfin. The orthotopic MatLyLu tumors were treated with vascular-targeting PDT as described in (A). Animals were i.v. injected with 10 mg/kg 2000 kDa FITC-dextran right before irradiation and imaged every 2 minutes for the FITC fluorescence during and after PDT. The images shown are right before PDT, immediately, 10 min and 30 min after PDT. Sizes of some blood vessels are labeled on the images. (C) The change of vascular permeability during and after vascular-targeting PDT with verteporfin. Vascular permeability change was determined by measuring the 2000 kDa FITC-dextran fluorescence intensity from the above intravital microscopic images and normalizing the after treatment intensity values to the pretreatment value. (D) The change of blood vessel size during and after vascular-targeting PDT with verteporfin. Sizes of four blood vessels on the above intravital microscopic images were measured and the percentages over pretreatment sizes are shown. (E) Immunohistochemical staining showing the difference in vessel morphology and structure between tumor peripheral and central blood vessels. Blood vessel pericyte marker α-small muscle actin (α-SMA) staining (red) indicates that peripheral vessels are generally bigger and have better pericyte coverage than central vessels. Note the existence of central necrosis. Blue shows the nuclei staining by Hoechst. (F) Non-invasive fluorescence imaging of tumor response after the vascular-targeting PDT with verteporfin. The EGFP-MatLyLu tumors were imaged with a whole body fluorescence imaging system before and after the vascular-targeting PDT showing tumor recurrence starting from 3 days after treatment. Images of control tumor receiving no treatment are also shown for comparison. Bar=10mm.

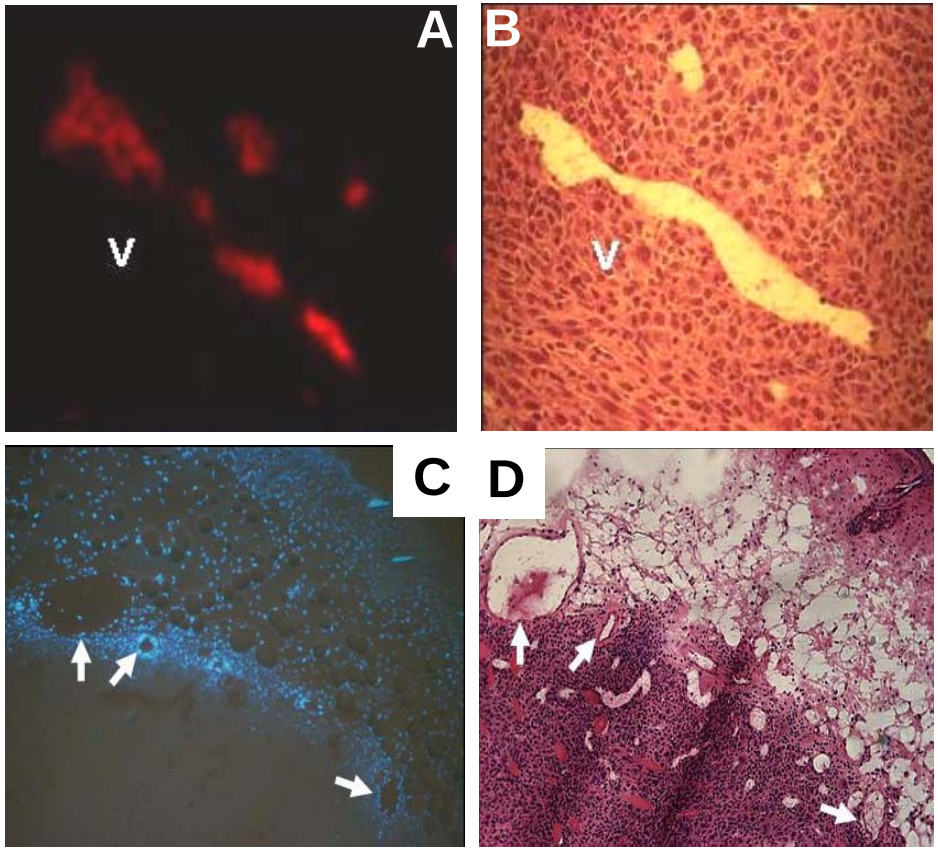
A
V
B
V
C
D
E
Control
Hypericin-PDT
TNP(30mg/kg)
Hypericin-PDT
+TNP (30mg/kg)
Tumor volume (mm3)
0
200
400
600
800
1000
0
2
4
6
8
5710
12
14
16
18
20
Days

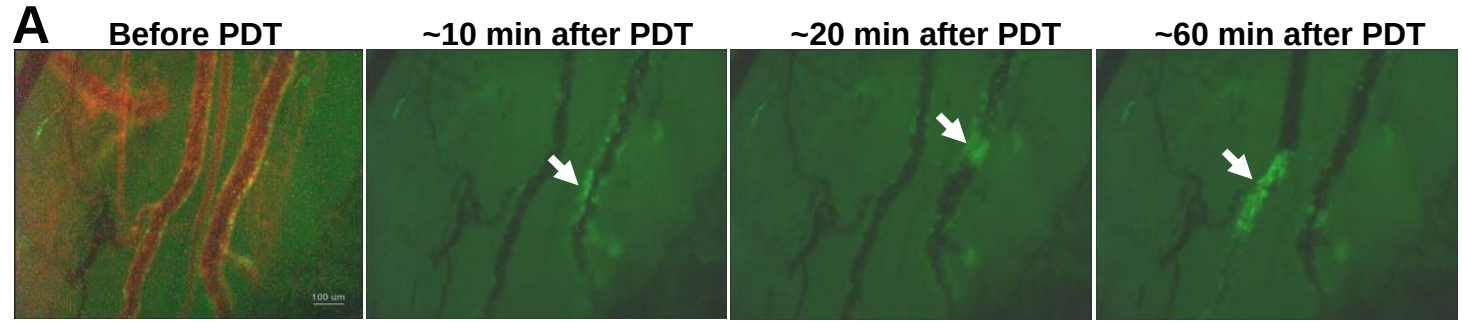
A
Before PDT
~10 min after PDT
~20 min after PDT
~60 min after PDT
100 um

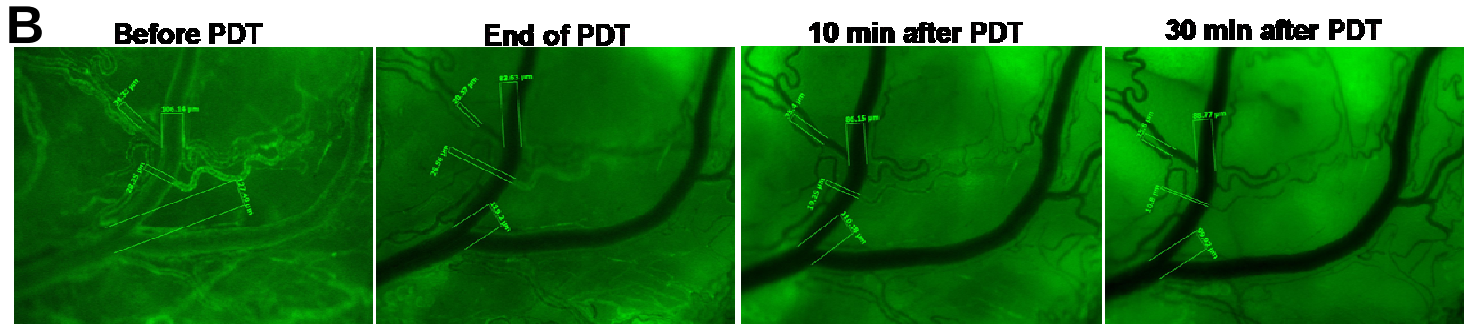
B
Before PDT
End of PDT
10 min after PDT
30 min after PDT

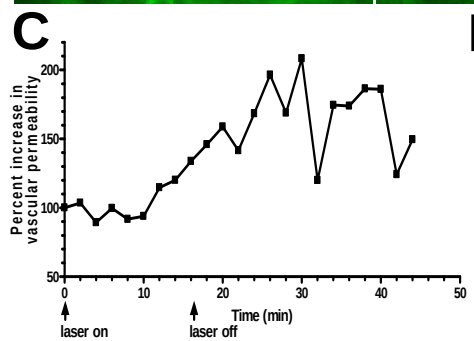
C
Percent increase in vascular permeability
200
150
100
50
0
10
20
30
40
50
Time (min)
laser on
laser off

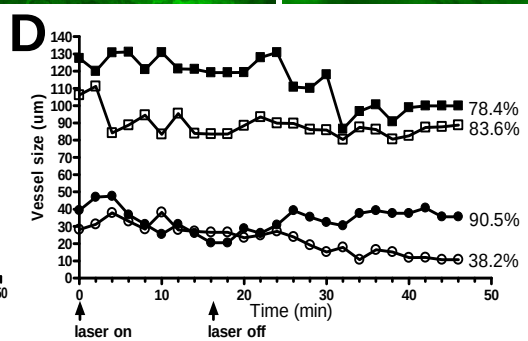
D
Vessel size (um)
140
130
120
110
100
90
80
70
60
50
40
30
20
10
0
78.4%
83.6%
90.5%
38.2%
Time (min)
laser on
laser off

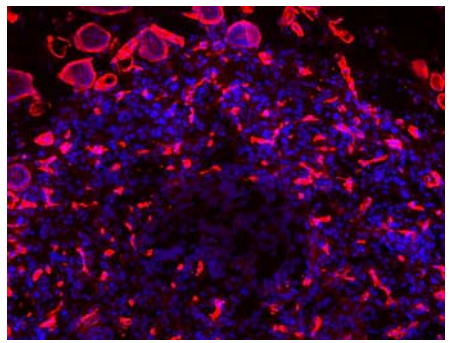
E

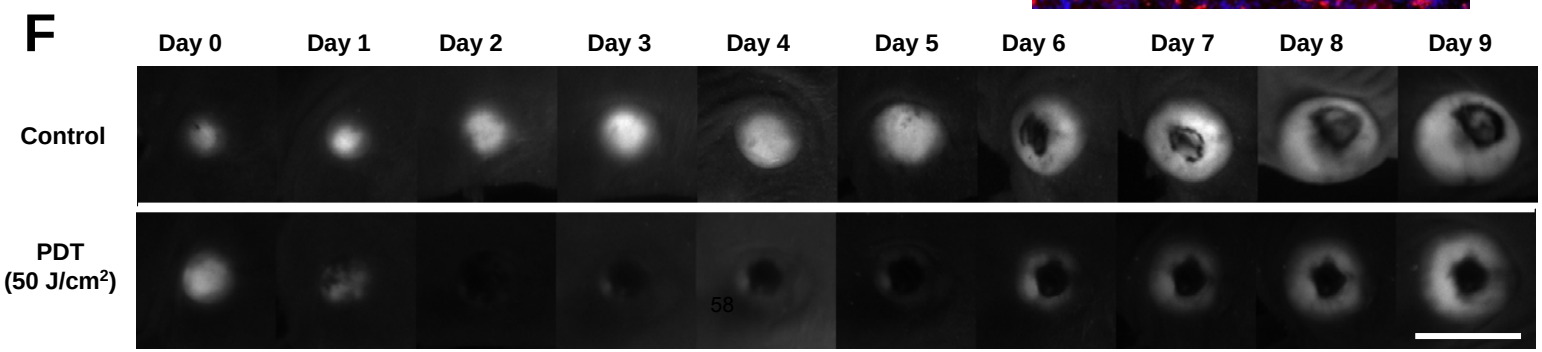
F
Day 0
Day 1
Day 2
Day 3
Day 4
Day 5
Day 6
Day 7
Day 8
Day 9
Control
PDT
(50 J/cm2)